Cell

A Large Intergenic Noncoding RNA Induced by p53 Mediates Global Gene Repression in the p53 Response

Maite Huarte,[1,2,*] Mitchell Guttman,[1,3] David Feldser,[3,4] Manuel Garber,[1] Magdalena J. Koziol,[1,2] Daniela Kenzelmann-Broz,[5,6] Ahmad M. Khalil,[1,2] Or Zuk,[1] Ido Amit,[1] Michal Rabani,[1] Laura D. Attardi,[5,6] Aviv Regev,[1,3] Eric S. Lander,[1,3,7] Tyler Jacks,[3,4] and John L. Rinn[1,2,*]

[1]The Broad Institute of MIT and Harvard, Cambridge, MA 02142, USA
[2]Department of Pathology, Beth Israel Deaconess Medical Center, Harvard Medical School, Boston, MA 02215, USA
[3]Department of Biology, Massachusetts Institute of Technology, Cambridge, MA 02139, USA
[4]The Koch Institute for Integrative Cancer Research, Cambridge, MA 02139, USA
[5]Department of Radiation Oncology
[6]Department of and Genetics
Stanford University School of Medicine, Stanford, CA 94305, USA
[7]Department of Systems Biology, Harvard Medical School, Boston, MA 02114, USA
*Correspondence: mhuarte@broadinstitute.org (M.H.), jrinn@broadinstitute.org (J.L.R.)
DOI 10.1016/j.cell.2010.06.040

SUMMARY

Recently, more than 1000 large intergenic noncoding RNAs (lincRNAs) have been reported. These RNAs are evolutionarily conserved in mammalian genomes and thus presumably function in diverse biological processes. Here, we report the identification of lincRNAs that are regulated by p53. One of these lincRNAs (lincRNA-p21) serves as a repressor in p53-dependent transcriptional responses. Inhibition of lincRNA-p21 affects the expression of hundreds of gene targets enriched for genes normally repressed by p53. The observed transcriptional repression by lincRNA-p21 is mediated through the physical association with hnRNP-K. This interaction is required for proper genomic localization of hnRNP-K at repressed genes and regulation of p53 mediates apoptosis. We propose a model whereby transcription factors activate lincRNAs that serve as key repressors by physically associating with repressive complexes and modulate their localization to sets of previously active genes.

INTRODUCTION

It has become increasingly clear that mammalian genomes encode numerous large noncoding RNAs (Mercer et al., 2009; Ponting et al., 2009; Mattick, 2009; Ponjavic et al., 2007). It has been recently reported the identification of more than 1000 large intergenic noncoding RNAs (lincRNAs) in the mouse genome (Carninci, 2008; Guttman et al., 2009). The approach to identify lincRNAs was by searching for a chromatin signature of actively transcribed genes, consisting of a histone 3-lysine 4 trimethylated (H3K4me3) promoter region and histone 3-lysine 36 trimethylation (H3K36me3) corresponding to the elongated transcript (Guttman et al., 2009). These lincRNAs show clear evolutionary conservation, implying that they are functional (Guttman et al., 2009; Ponjavic et al., 2007).

In an attempt to understand the potential biological roles of lincRNAs, a method to infer putative function based on correlation in expression between lincRNAs and protein-coding genes was developed. These studies led to preliminary hypotheses about the involvement of lincRNAs in diverse biological processes, from stem cell pluripotency to cell-cycle regulation (Guttman et al., 2009). In particular, we observed a group of lincRNAs that are strongly associated with the p53 transcriptional pathway. p53 is an important tumor suppressor gene involved in maintaining genomic integrity (Vazquez et al., 2008). In response to DNA damage, p53 becomes stabilized and triggers a transcriptional response that causes either cell arrest or apoptosis (Riley et al., 2008).

The p53 transcriptional response involves both activation and repression of numerous genes. While p53 is known to transcriptionally activate numerous genes, the mechanisms by which p53 leads to gene repression have remained elusive. We recently reported evidence that many lincRNAs are physically associated with repressive chromatin modifying complexes and suggested that they may serve as repressors in transcriptional regulatory networks (Khalil et al., 2009). We therefore hypothesized that p53 may repress genes in part by directly activating lincRNAs, which in turn regulate downstream transcriptional repression.

Here, we show that lincRNAs play a key regulatory role in the p53 transcriptional response. By exploiting multiple independent cell-based systems, we identify lincRNAs that are transcriptional targets of p53. Moreover, we find that one of these p53-activated lincRNAs—termed lincRNA-p21—serves as a transcriptional repressor in the p53 pathway and plays a role in triggering apoptosis. We further demonstrate that lincRNA-p21 binds to

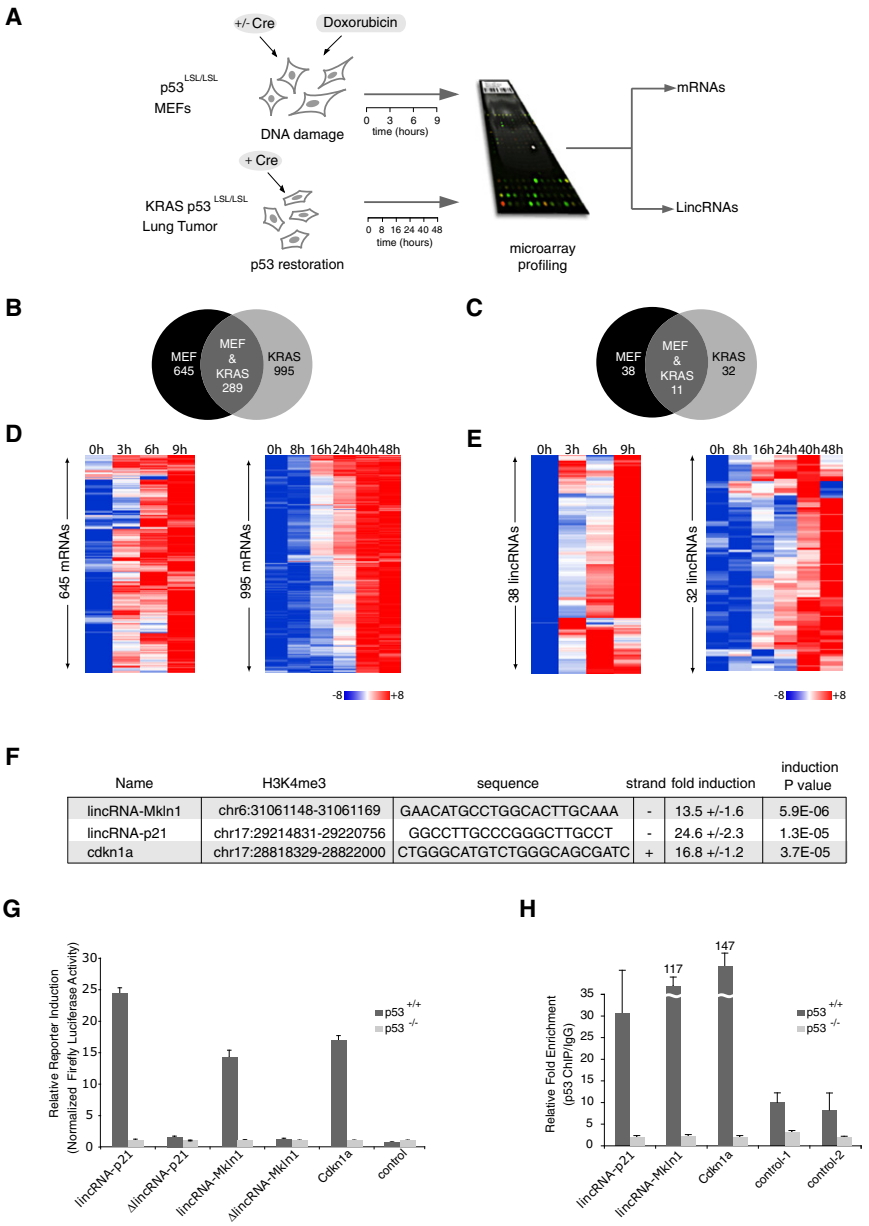

F

Name	H3K4me3	sequence	strand	fold induction	induction P value
lincRNA-Mkln1	chr6:31061148-31061169	GAACATGCCTGGCACTTGCAAA	-	13.5 +/-1.6	5.9E-06
lincRNA-p21	chr17:29214831-29220756	GGCCTTGCCCGGGCTTGCCT	-	24.6 +/-2.3	1.3E-05
cdkn1a	chr17:28818329-28822000	CTGGGCATGTCTGGGCAGCGATC	+	16.8 +/-1.2	3.7E-05

Figure 1. Several LincRNAs Are p53 Transcriptional Targets

(A) Experiment layout to monitor p53-dependent transcription. p53-restored (+Cre) or not restored (−Cre) p53$^{LSL/LSL}$ MEFs were treated with 500 nM dox for 0, 3, 6, and 9 hr (upper left). KRAS (p53$^{LSL/LSL}$) tumor cells were treated with hydroxytamoxifen for p53 restoration for 0, 8, 16, 24, 40, or 48 hr (lower left). RNA was subjected to microarray analysis of mRNAs and lincRNAs.

(B and C) Venn diagrams showing the number of shared and distinct mRNAs (B) or lincRNAs (C) induced in a p53-dependent manner in the MEF or KRAS systems.

(D and E) mRNAs (D) and lincRNAs (E) activated by p53 induction (FDR < 0.05) in MEF or KRAS system. Colors represent transcripts above (red) or below (blue) the global median scaled to 8-fold activation or repression, respectively.

(F) Promoter region, conserved p53 binding motif, promoter orientation, and p53-dependent fold induction in reporter assays of lincRNA promoters induced in a p53-dependent manner (values are average of at least three biological replicates [±STD]; p values are determined by t test).

(G) p53-dependent induction of lincRNA promoters requires the consensus p53 binding elements. Relative firefly luciferase expression driven by promoters with p53 consensus motif (lincRNA-p21, lincRNA-Mkln1) or with deleted motif (ΔlincRNA-p21 and ΔlincRNA-Mkln1) in p53-restored p53$^{LSL/LSL}$ (p53$^{+/+}$) or p53$^{LSL/LSL}$ (p53$^{-/-}$) cells. Values are relative to p53$^{-/-}$ and normalized by renilla levels (average of three replicates ±STD).

(H) p53 specifically binds to p53 motifs in lincRNA promoters. p53 ChIP enrichment in p53$^{+/+}$ and p53$^{-/-}$ MEFs on regions with p53 motifs (lincRNA-p21, lincRNA-Mkln1, Cdkn1a) or two irrelevant regions (controls). Enrichment values are relative to IgG and average of 3 replicates (±STD).

See also Figure S1 and Table S1.

hnRNP-K. This interaction is required for proper localization of hnRNP-K and transcriptional repression of p53-regulated genes. Together, these results reveal insights into the p53 transcriptional response and lead us to propose that lincRNAs may serve as key regulatory hubs in transcriptional pathways.

RESULTS

Numerous LincRNAs Are Activated in a p53-Dependent Manner

As a first attempt to dissect the functional mechanisms of lincRNAs, we focused on a strong association in the expression patterns of certain lincRNAs and genes in the p53 pathway (Guttman et al., 2009). In order to determine whether these lincRNAs are regulated by p53, we employed two independent experimental systems that allow us to monitor gene expression changes at different times after p53 induction (Ventura et al., 2007).

The first system uses mouse embryonic fibroblasts (MEFs) derived from mice where the endogenous p53 locus is inactivated by insertion of a transcriptional termination site flanked by loxP sites (LSL) in the first intron. This endogenous *p53* locus (p53 $^{LSL/LSL}$) is restorable by removal of the stop element by Cre recombination (Ventura et al., 2007). The p53 $^{LSL/LSL}$ MEFs were treated with AdenoCre virus expressing the Cre recombinase to reconstitute the normal p53 allele or AdenoGFP control virus to maintain the inactive p53 $^{LSL/LSL}$ allele. Then we compared the transcriptional response between the p53-reconstituted and p53 $^{LSL/LSL}$ MEFs after 0, 3, 6, and 9 hr of DNA damage treatment with doxorubicin (we will refer to this system as "MEFs") (Figure 1A). The second system uses a lung tumor cell line

derived from mice expressing an oncogenic K-Ras mutation (K-RasG12D) and a restorable *p53* knockout allele (p53 $^{LSL/LSL}$), similar to that described above (D.F. and T.J., unpublished data). We compared the transcriptional response at different times (0, 8, 16, 24, 40, and 48 hr) after restoration of p53 expression by Cre recombination (Experimental Procedures) (we will refer to this system as "KRAS") (Figure 1A).

To assess the transcriptional responses in each of these systems, we isolated total RNA at each time point before and after *p53* restoration and performed DNA microarray analysis to monitor protein-coding gene expression levels. In the MEF system and KRAS systems, we identified a total of 1067 (645 activated, 422 repressed) and 1955 (995 activated, 960 repressed) genes, respectively, that were regulated in a p53-dependent manner (false discovery rate [FDR] < 0.05) (Figures 1B and 1D and Table S1, parts A and B, available online). The sets of p53-induced genes identified in the two systems showed significant ($p < 10^{-8}$) overlap, including such canonical p53 targets as *Cdnk1a*, *Mdm2*, *Perp*, and *Fas* (Table S1, parts A and B). There are also a number of p53-induced genes unique to each system, likely reflecting specific properties of each cell-type (Levine et al., 2006) (Figure S1C and Table S1, parts A and B).

Functional analysis of the classes of genes that are enriched among the genes regulated by p53 in both the MEF and KRAS systems showed strong enrichment for known p53-regulated processes, such as the cell cycle and apoptosis (Figures S1A and S1B). Moreover, gene set enrichment analysis (GSEA) (Subramanian et al., 2005) of previously published microarray analyses revealed a significant overlap with the p53 regulated genes identified here (Table S1, parts H and I). Together these results demonstrate that these two systems are largely reflective of canonical p53 transcriptional responses.

We next examined lincRNAs regulated by p53 in these two systems across the same time course, by analogously using a custom tiling microarray representing 400 lincRNAs and analyzing the data with previously described statistical methods (Guttman et al., 2009) (Experimental Procedures). We found 38 and 32 lincRNAs induced by p53 in the MEF and KRAS systems, respectively (Figures 1C and 1E and Table S1, parts C–G). Interestingly, 11 lincRNAs were induced by p53 in both model systems (Figure 1C and Table S1, part C), many more than expected by chance ($p < 10^{-6}$). These results confirm that, in a manner similar to canonical p53 protein coding gene targets, numerous lincRNAs are temporally regulated by p53.

LincRNAs Are Direct Transcriptional Targets of p53

We sought to identify lincRNAs that might be canonical p53 target genes. As a first approach, we examined the promoters of p53-induced lincRNA for enrichment of evolutionarily conserved p53-binding motifs (Garber et al., 2009) (Extended Experimental Procedures). The promoters of the p53-induced lincRNAs were highly enriched for conserved p53 motifs relative to the promoters of all lincRNAs ($p < 0.01$). We selected two lincRNAs whose promoter regions contain highly conserved canonical p53-binding motifs (el-Deiry et al., 1992; Funk et al., 1992); we termed these *lincRNA-p21* and *lincRNA-Mkln1* (with the names referring to the neighboring gene). We next performed transcriptional reporter assays for these lincRNAs. Specifically, we cloned their promoters (as defined by the H3K4me3 peaks [Guttman et al., 2009]) into a luciferase reporter vector (Experimental Procedures) and transfected the constructs along with a vector to normalize transfection efficiency. Both promoters showed significant induction of firefly luciferase in p53-wild-type but not in p53 null cells ($p < 0.01$) (Figures 1F and 1G).

To determine whether the canonical p53-binding motif is required for the observed transactivation, we repeated these experiments in the absence of the p53-binding motif. Mutant promoters resulted in the abolition of the observed transactivation for both lincRNA-p21 and lincRNA-Mkln1 in $p53^{+/+}$ cells (Figure 1F). Finally, we performed chromatin immunoprecipitation (ChIP) experiments to determine whether p53 directly binds to the sites containing the consensus motifs in vivo. Indeed, p53 is bound to the site containing the consensus motif in the promoters of both *lincRNA-p21* and *lincRNA-Mkln1* in $p53^{+/+}$ but not $p53^{-/-}$ MEFs treated with doxorubicin, and it is not enriched at negative control sites of irrelevant regions (Figure 1H and Extended Experimental Procedures). Together, these results demonstrate that *lincRNA-p21* and *lincRNA-Mkln1* are bona fide p53 transcriptional targets.

LincRNA-p21 Is Induced by p53 in Different Cell Systems

We were intrigued by the p53 transcriptional target *lincRNA-p21*, which resides ~15 Kb upstream of the gene encoding the critical cell-cycle regulator *Cdkn1a* (also known as *p21*), a canonical transcriptional target of p53 (Riley et al., 2008) (Figures 2A–2C, Figure S2A, and Table S1, parts C–E). Given the proximity of *lincRNA-p21* to the *Cdkn1a* gene, we sought to ensure that the lincRNA transcript is distinct from that of the *Cdkn1a* gene. To this end, we cloned the full-length transcriptional unit of lincRNA-p21 using the 5′ and 3′ RACE method (Schaefer, 1995); the transcript contains two exons comprising 3.1 Kb (Figure 2B). In support of lincRNA-p21 being an independent transcript, *lincRNA-p21* is transcribed in the opposite orientation from the *Cdkn1a* gene. Furthermore, the analysis of chromatin structure in mouse embryonic stem cells (mESCs) (Mikkelsen et al., 2007) indicates that these are distinct genes with distinct promoters (Figure S2A).

We next examined the transcriptional regulation of *lincRNA-p21* in two additional cancer-derived cell lines. Specifically, we irradiated $p53^{LSL/LSL}$ mice to induce lymphomas and sarcomas and then restored p53 expression in tumor-derived cells (Experimental Procedures) (Ventura et al., 2007). In cells derived in both tumor types, lincRNA-p21 was strongly induced after p53 restoration. Moreover, the induction of lincRNA-p21 followed similar kinetics as those of p53 and *Cdnk1a*, consistent with *lincRNA-p21* being a primary transcriptional target of p53 (Figure 2D and Figure S2B).

We further investigated the orthologous *lincRNA-p21* locus in the human genome. We first mapped the promoter (H3K4me3 domain) of *lincRNA-p21* to human genome. Interestingly, this region corresponds to one of four intergenic p53-binding sites identified from a study by Wei et al. (2006) (Figure 2B) performing p53 ChIP followed by sequencing. Next, we mapped the lincRNA-p21 exonic structures to the human genome to determine whether this region is expressed and induced by DNA

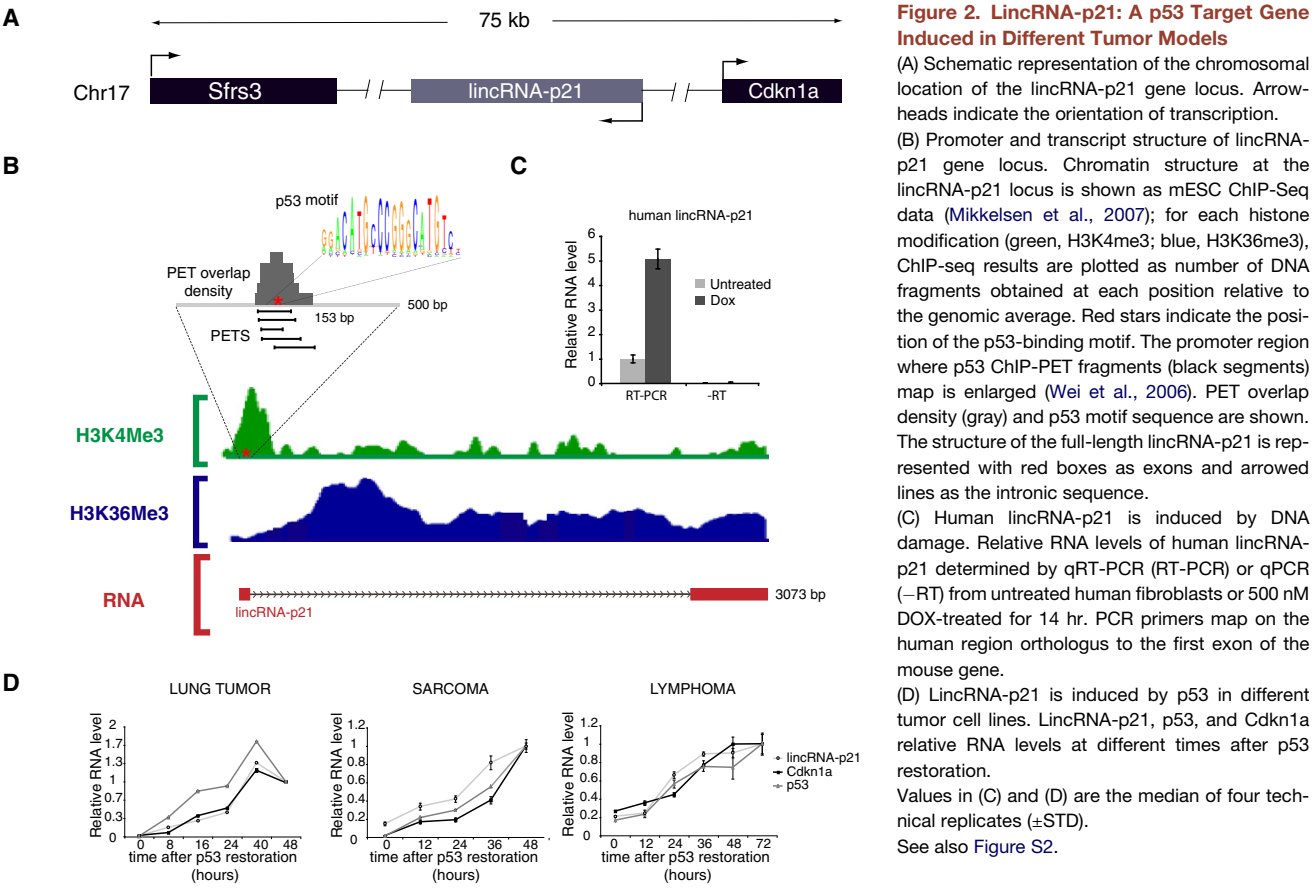

Figure 2. LincRNA-p21: A p53 Target Gene Induced in Different Tumor Models

(A) Schematic representation of the chromosomal location of the lincRNA-p21 gene locus. Arrowheads indicate the orientation of transcription.

(B) Promoter and transcript structure of lincRNA-p21 gene locus. Chromatin structure at the lincRNA-p21 locus is shown as mESC ChIP-Seq data (Mikkelsen et al., 2007); for each histone modification (green, H3K4me3; blue, H3K36me3), ChIP-seq results are plotted as number of DNA fragments obtained at each position relative to the genomic average. Red stars indicate the position of the p53-binding motif. The promoter region where p53 ChIP-PET fragments (black segments) map is enlarged (Wei et al., 2006). PET overlap density (gray) and p53 motif sequence are shown. The structure of the full-length lincRNA-p21 is represented with red boxes as exons and arrowed lines as the intronic sequence.

(C) Human lincRNA-p21 is induced by DNA damage. Relative RNA levels of human lincRNA-p21 determined by qRT-PCR (RT-PCR) or qPCR (−RT) from untreated human fibroblasts or 500 nM DOX-treated for 14 hr. PCR primers map on the human region orthologus to the first exon of the mouse gene.

(D) LincRNA-p21 is induced by p53 in different tumor cell lines. LincRNA-p21, p53, and Cdkn1a relative RNA levels at different times after p53 restoration.

Values in (C) and (D) are the median of four technical replicates (±STD).

See also Figure S2.

damage in human fibroblasts. Indeed, qRT-PCR showed that the orthologous 5′ exon region (adjacent to observed p53 ChIP binding site by Wei et al.) of human *lincRNA-p21* is expressed and strongly induced in human fibroblasts upon DNA damage (Figure 2C and Extended Experimental Procedures).

Collectively, these results provide evidence that both the human and mouse *lincRNA-p21* promoters are bound by p53 resulting in transcriptional activation in response to DNA damage. Moreover, *lincRNA-p21* is induced by p53 in diverse biological contexts, including multiple different tumor types (Figure 2D and Figure S2B), suggesting that lincRNA-p21 plays a role in the p53 pathway.

LincRNA-p21 as a Repressor in the p53 Pathway

We next investigated the consequence of the loss of lincRNA-p21 function in the context of the p53 response. We reasoned that, if lincRNA-p21 plays a role in carrying out the p53 transcriptional response, then inhibition of lincRNA-p21 would show effects that overlap with inhibition of p53 itself. To test this hypothesis, we performed RNA interference (RNAi)-mediated knockdown of lincRNA-p21 and p53 separately and monitored the resulting changes in mRNA levels by DNA microarray analysis.

Toward this end, we first designed a pool of small interfering RNA (siRNA) duplexes targeting lincRNA-p21, a pool targeting p53 or nontargeting control sequences. We validated that each pool was effective at knocking down its intended target genes in $p53^{LSL/LSL}$ restored MEFs (Figures 3A and 3B). We then used microarray analysis to examine the broader transcriptional consequences of knockdown of p53 and lincRNA-p21. We identified 1520 and 1370 genes that change upon knockdown of p53 and lincRNA-p21, respectively (relative to nontargeting control siRNA, FDR < 0.05). We observed a remarkable overlap of 930 genes in both the lincRNA-p21 and p53 knockdowns, vastly more than would be expected by chance ($p < 10^{-200}$) (Figure 3C, Figure S3A, and Table S2). Strikingly, 80% (745/930) of the common genes are derepressed in response to both p53 and lincRNA-p21 knockdown, much higher proportion than expected by chance ($p < 10^{-10}$) (Figure 3C and Table S2) when compared to all genes affected by the p53 knockdown (Figure S3A). This observation suggests that lincRNA-p21 participates in downstream p53 dependent transcriptional repression.

To demonstrate that the observed derepression upon lincRNA-p21 knockdown is indeed p53 dependent and is not due to off target effects of the RNAi-mediated knockdown, we performed several additional experiments and analyses. First, we repeated the knockdown experiments with four individual siRNAs targeting lincRNA-p21, transfected separately rather than in a pool and confirmed the derepression effect on select target genes (Figure S3F and Table S2). Second, we confirmed that the same genes that were derepressed in the lincRNA-p21 and p53 knockdown experiments correspond to genes that are

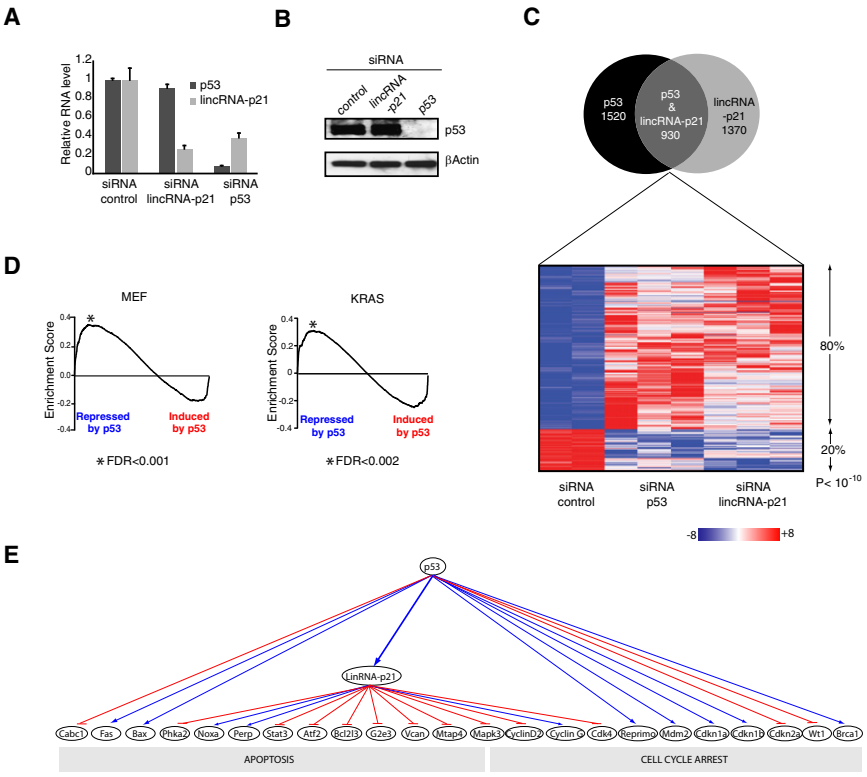

Figure 3. LincRNA-p21 Is a Global Repressor of Genes in the p53 Pathway

(A) RNAi-mediated knockdown of lincRNA-p21 and p53. Relative RNA levels determined by qRT-PCR in p53-reconstituted $p53^{LSL/LSL}$ MEFs transfected with the indicated siRNAs and treated with DOX (median of four technical replicates ±STD).

(B) p53 protein levels after lincRNA-p21 and p53 knockdown from cells treated as in (A). βActin levels are shown as loading control.

(C) Many genes are corepressed by lincRNA-p21 and p53. Top: Venn diagram of differentially expressed genes (FDR < 0.05) upon p53 knockdown (left) or lincRNA-p21 knockdown (right); cells were treated as in (A) and subjected to microarray analysis. Bottom: expression level of genes in lincRNA-p21 and p53 siRNA-treated cells relative to control siRNA experiments. Expression values are displayed in shades of red or blue relative to the global median expression value across all experiments (linear scale).

(D) Genes derepressed by lincRNA-p21 and p53 knockdown overlap with the genes repressed by p53 restoration in the MEF and KRAS systems. The black line represents the observed enrichment score profile of genes in the lincRNA-p21/p53 derepressed gene set to the MEF or KRAS gene sets, respectively.

(E) Genes corregulated by lincRNA-p21 and p53 are part of the p53 biological response. Examples of genes affected by lincRNA-p21 and/or p53 siRNA-knockdown (FDR < 0.05). Downregulated and upregulated genes are indicated with blue arrows and red lines respectively.

See also Figure S3 and Table S2.

normally repressed upon p53 induction in both the KRAS and MEF systems, in the absence of RNAi treatment (GSEA FDR < 0.002) (Figure 3D). Third, we demonstrated that enforced expression of lincRNA-p21 (Experimental Procedures) also perturbed the expression of genes that are normally regulated by p53 in both the KRAS and MEF systems (GSEA FDR < 0.01) (Figure S3H). Finally, we repeated the siRNA experiments in the absence of p53 (dox/-AdCre) and demonstrated that derepression of these genes did not occur upon siRNA-mediated knockdown in the absence of p53 (Figure S3I). Collectively, these results indicate that lincRNA-p21 acts to repress many genes in p53-dependent transcriptional response.

lincRNA-p21 Regulates Apoptosis

The activation of the p53 pathway has two major phenotypic outcomes: growth arrest and apoptosis (Levine et al., 2006). Consistent with this, our microarray analysis demonstrates that p53 and lincRNA-p21 both regulate a number of apoptosis and cell-cycle regulator genes (Figure 3E, Figure S3G, and Table S2, parts A and B). Thus, we aimed to determine the physiological role of lincRNA-p21 in these processes.

Toward this end, we used RNAi-mediated knockdown of lincRNA-p21 in dox-treated or untreated primary MEFs. We similarly performed RNAi-mediated knockdown of p53 (as a positive control) or used the nontargeting siRNA pool (as a negative control) under the same conditions. We observed a significant increase in viability after DNA damage of cells treated with siRNAs targeting either lincRNA-p21 or p53 compared to those treated with the control siRNA pool (Figures 4A and 4B). The increase in viability was greater for knockdown of p53, but was still highly significant for knockdown of lincRNA-p21 ($p < 0.01$). We observed similar results when using three individual siRNA duplexes targeting lincRNA-p21, as well as two different control siRNA pools (Figure 4B and Figures S4A–S4C). These results suggest that lincRNA-p21 plays a physiological role in regulating cell viability upon DNA damage in this system, although they do not discriminate whether the effect is due to misregulation of the cell cycle or apoptosis.

To distinguish between these two possibilities, we first examined whether cell-cycle regulation in response to DNA damage is affected by knockdown of p53 and lincRNAp-21. Specifically, we assayed 5-bromo-2-deoxyuridine (BrdU) incorporation and propidium iodide staining of the cells by fluorescence-activated cell sorting (FACS) analysis. Consistent with the ability of p53 to inhibit cell-cycle progression, knockdown of p53 caused a significant increase in BrdU incorporation in response to DNA damage ($p < 0.01$). In contrast, knockdown of lincRNA-p21 showed no significant changes in either BrdU levels or in the percentages of cells in any of the cell-cycle phases (S, G1, or G2) with or without dox treatment (Figure 4C). These results suggest that lincRNA-p21 does not substantially contribute to cell-cycle arrest upon DNA damage.

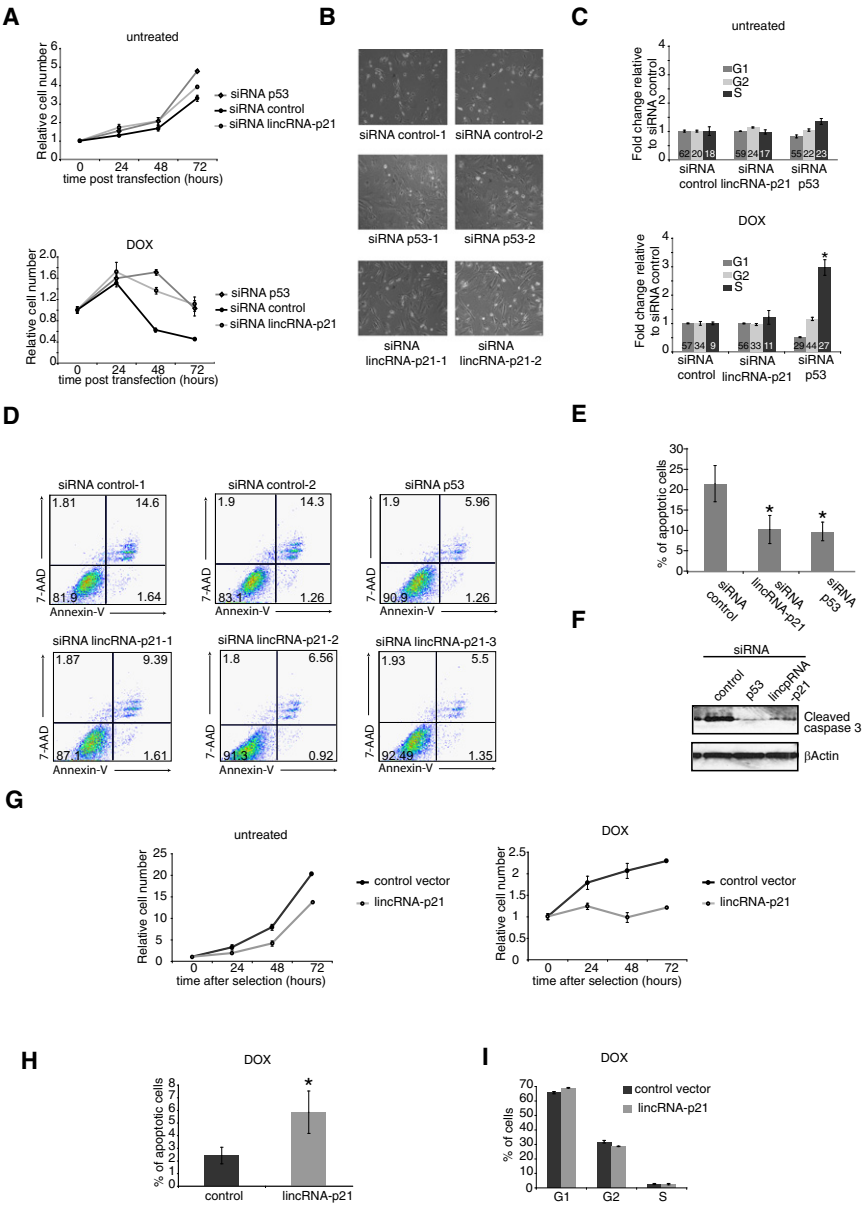

Figure 4. LincRNA-p21 Is Required for Proper Apoptotic Induction

(A) Increased cell viability of lincRNA-p21-depleted cells. Relative number of siRNA-transfected MEFs treated with 400 nM DOX from 24 hr after transfection (right) or untreated (left) determined by MTT assay.

(B) Knockdown of lincRNA-p21 with individual siRNAs increases cell viability. Images of MEFs treated with different individual siRNAs after 48 hr of DOX treatment (72 hr after transfection).

(C) LincRNA-p21 knockdown doesn't affect cell-cycle regulation. Relative cell numbers in each cell-cycle phase determined by FACS of BrdU incorporation and PI staining of MEFs treated as in (A). Numbers inside bars represent percentages of cells in each phase.

(D) LincRNA-p21 knockdown causes a decrease in cellular apoptosis. p53-reconstituted $p53^{LSL/LSL}$ MEFs transfected with three individual siRNAs targeting lincRNA-p21 (bottom), two independent control siRNAs (upper left and middle) or a siRNA pool targeting p53 (upper right). Twenty-four hours after transfection, cells were treated with 400 nM doxorubicin and 14 hr later were harvested and subjected to FACS analysis. The x axis represents Annexin-V and the y axis 7-AAD staining. The percentage of cells in each quadrant is indicated.

(E) Decreased apoptosis caused by lincRNA-p21 knockdown. Percentage of Annexin-V-positive cells (FACS) at 38 hr after transfection (14 hr of 400 nM DOX treatment) in MEFs treated as in (A).

(F) LincRNA-p21 knockdown in p53-reconstituted $p53^{LSL/LSL}$ MEFs causes decrease in Caspase 3 cleavage. Levels of cleaved Caspase 3 or control βActin in p53 reconstituted-$p53^{LSL/LSL}$ MEFs treated with the indicated siRNA pools and 500 nM DOX for 14 hr.

(G) Decreased cell viability caused by lincRNA-p21 overexpression. Relative numbers of LKR cells overexpressing lincRNA-p21 or control plasmid determined by MTT assay.

(H) Overexpression of lincRNA-p21 causes cellular apoptosis under DNA damage induction. Percentage of Annexin-V-positive LKR cells overexpressing lincRNA-p21 or control vector treated with 500 nM DOX.

(I) LincRNA overexpression doesn't affect cell-cycle regulation. Cell-cycle analysis of DOX-treated LKR cells overexpressing lincRNA-p21 or control plasmid.

All values are the average of 3 biological replicates (±STD). * $p < 0.01$ relative to controls.

Also see Figure S4.

We then examined the impact of lincRNA-p21 and p53 knockdowns on apoptosis. To this end, we assayed the proportion of the cell population undergoing apoptosis by measuring Annexin-V by FACS analysis. We observed a significant decrease in the number of apoptotic cells after DNA damage in both the lincRNA-p21 and p53 depleted cells relative to the siRNA control ($p < 0.01$) (Figures 4D and 4E). We also observed a decrease in Caspase 3 cleavage after knockdown of both p53 or lincRNA-p21, relative to controls (Figure 4F). We next sought to determine whether, conversely to lincRNA-p21 knockdown, the enforced expression of lincRNA-p21 would result in an increased apoptosis. Indeed, lincRNA-p21 overexpression in a lung cancer cell line harboring a KRAS mutation (referred to as LKR) and in NIH/3T3 MEFs caused a significant decrease in cell viability (Experimental Procedures, Figure 4G, and Figure S4E). This decrease in viability was due to increased apoptosis in response to DNA damage ($p < 0.01$) and not to an effect in cell-cycle regulation (Figures 4H and 4I and Figure S4G). Together, these results demonstrate a reproducible and similar reduction of apoptotic cells in response to DNA damage in both lincRNA-p21 and p53 knockdown experiments.

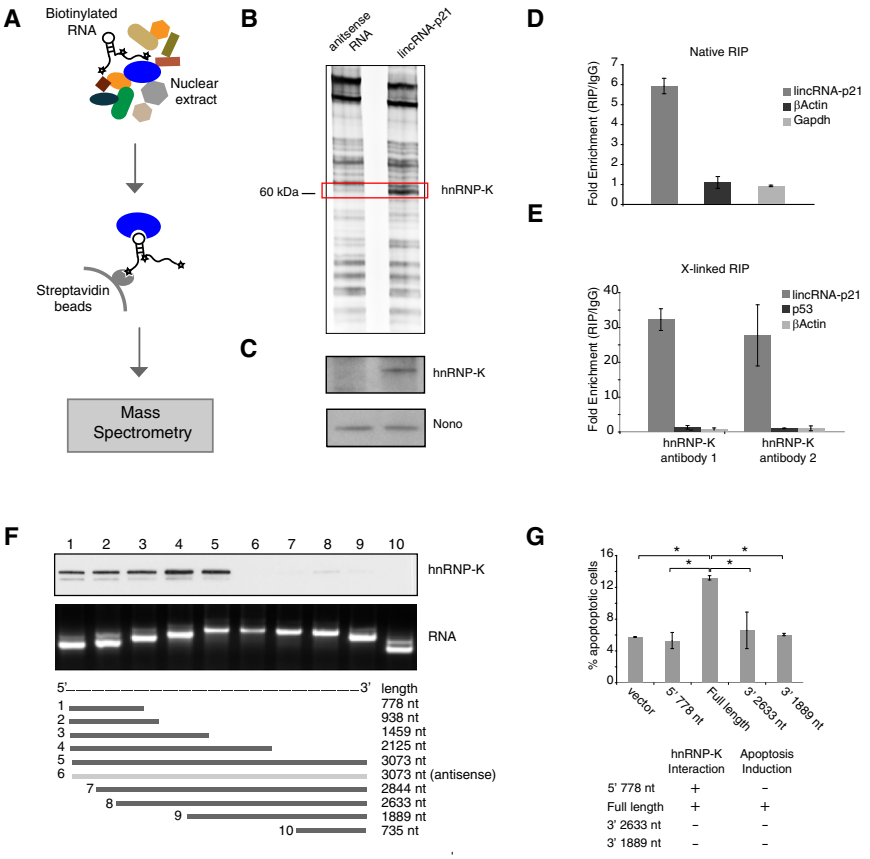

Figure 5. LincRNA-p21 Physically Interacts with hnRNP-K

(A) Schematic representation of RNA pulldown experiments to identify associated proteins. Biotinylated lincRNA-p21 or antisense RNA were incubated with nuclear extracts, targeted with streptavidin beads, washed, and associated proteins resolved in a gel. Specific bands were cutout and identified by mass spectrometry.

(B) LincRNA-p21 and hnRNP-K specifically interact in vitro. SDS-PAGE gel of proteins bound to lincRNA-p21 (right lane) or antisense RNA (left lane). The highlighted region was submitted for mass spectrometry identifying hnRNP-K as the band unique to lincRNA-p21.

(C) Western blot analysis of the specific association of hnRNP-K with lincRNA-p21. A nonspecific protein (NONO) is shown as a control.

(D) Association between endogenous lincRNA-p21 and hnRNP-K in the nucleus of DNA damaged MEFs in native conditions. RNA Immunoprecipitation (RIP) enrichment is determined as RNA associated to hnRNP-K IP relative to IgG control.

(E) Physical association between lincRNA-p21 and hnRNP-K after chemical crosslinking of life cells. hnRNP-K was immunoprecipitated from nuclear extracts of formaldehyde-crosslinked DNA-damaged MEFs, and associated RNAs were detected by RT-qPCR. The relative enrichment is calculated as in (D) and is the median of three technical replicates of a representative experiment (±STD).

(F) LincRNA-p21 binds hnRNP-K through its 5′ terminal region. RNAs corresponding to different fragments of lincRNA-p21 or its antisense sequence (middle and bottom) were treated as in (A) and associated hnRNP-K was detected by western blot (top).

(G) Percentage of Annexin-V-positive LKR cells overexpressing the indicated lincRNA-p21 fragments or empty vector as control (average of three replicates [±STD]). * $p < 0.001$.

See also Figure S5.

Although MEFs typically respond to DNA damage by undergoing cell-cycle arrest rather than apoptosis (Kuerbitz et al., 1992), several additional lines of evidence are consistent with the observed apoptosis phenotype in response to knockdown on p53 and lincRNA-p21. First, certain critical cell-cycle regulators, such as *Cdkn1a/p21*, *Cdkn2a*, and *Reprimo*, are regulated by p53 but not lincRNA-p21. For example, knockdown of lincRNA-p21 perturbs neither the transcript levels of *Cdkn1a/p21* nor the protein stability (Figure S3E); this may explain why lincRNA-p21 knockdown is insufficient to cause a cell-cycle phenotype, yet the p53 knockdown is. Second, we observed that both lincRNA-p21 and p53 knockdowns resulted in the repression of apoptosis genes (*Noxa* and *Perp*) and derepression of cell survival genes (*Bcl2l3*, *Stat3*, and *Atf2*, among others) (Figure 3E and Table S2). Moreover, the decrease of apoptotic cells in response to knockdown of lincRNA-p21 was comparable to that caused by knockdown of p53 (Figures 4D and 4E and Figures S4D and S4E). Third, the apoptosis phenotype is dependent on the dosage of dox-induced DNA damage (Figure S4D). Thus, the apoptosis response is both p53 dependent and lincRNA-p21 dependent, with this dependence confirmed in multiple cell types and conditions (Figures 4B, 4D, 4F, and 4H and Figures S4A–S4C). Collectively, these observations demonstrate that lincRNA-p21 plays an important role in the p53-dependent induction of cell death.

LincRNA-p21 Functions through Interaction with hnRNP-K

We next wanted to investigate the mechanism by which lincRNA-p21 mediates transcriptional repression. We have recently reported that many lincRNAs regulate gene expression through their interaction with several chromatin regulatory complexes (Khalil et al., 2009). Thus, we hypothesized that lincRNA-p21 could affect gene expression in a similar manner.

To test this, we first performed nuclear fractionation experiments and confirmed that lincRNA-p21 is enriched in the nucleus (Figure S5A). We next sought to identify proteins that are associated with lincRNA-p21 by an RNA-pulldown experiment. Specifically, we incubated in vitro-synthesized biotinylated lincRNA-p21 and antisense lincRNA-p21 transcripts (negative control) with nuclear cell extracts and isolated coprecipitated proteins with streptavidin beads (Experimental Procedures). We resolved the RNA-associated proteins on a SDS-PAGE gel, cut out the bands specific to lincRNA-p21, and subjected them to mass spectrometry (Figures 5A and 5B). In all six biological replicates, mass-spectrometry analysis identified heterogeneous nuclear

ribonucleoprotein K (hnRNP-K) as specifically associated with the sense (but not antisense) strand of lincRNA-p21. We independently verified this interaction by western blot analysis (Figure 5C). hnRNP-K has been shown to play various roles in the p53 pathway (Kim et al., 2008; Moumen et al., 2005). Interestingly, among these roles, Kim et al. (2008) demonstrated that hnRNP-K is a component of a repressor complex that acts in the p53 pathway, consistent with our evidence that lincRNA-p21 plays a role in global repression in this pathway.

To further validate the interaction between lincRNA-p21 and hnRNP-K in our cell-based systems, we performed RNA immunoprecipitation (RIP) with an antibody against hnRNP-K from nuclear extracts of MEFs subjected to DNA damage. We observed an enrichment of lincRNA-p21 (but not other unrelated RNAs) with hnRNP-K antibody as compared to the nonspecific antibody (IgG control) (Figure 5D). We further performed analogous RIP experiments with formaldehyde crosslinked cells followed by stringent washing conditions (Ule et al., 2005) to rule out potential nonspecific interactions. Consistent with a bona fide interaction, we observed a greater and very significant enrichment of lincRNA-p21 in the hnRNP-K RIP relative to the IgG control RIP with two hnRNP-K different antibodies (Figure 5E).

We further performed deletion-mapping experiments to determine whether hnRNP-K interacts within a specific region of lincRNA-p21. To this end, we carried out RNA pulldown experiments with truncated versions of lincRNA-p21 followed by western blot detection of bound hnRNP-K. These analyses identified a 780 nt region at the 5′ end of lincRNA-p21 required for the interaction with hnRNP-K (Figure 5F). Interestingly, RNA folding analyses of this region based on sequence conservation and compensatory changes across 14 mammalian species (Hofacker, 2003) predict a highly stable 280 nt structure of lincRNA-p21 with deep evolutionary conservation (Figures S5B and S5C). Together, the RNA pulldown, native RIP, crosslinked RIP, and deletion mapping results demonstrate a specific association between hnRNP-K and lincRNA-p21.

We next sought to determine the functional relevance of the interaction between lincRNA-p21 and hnRNP-K. To do so, we monitored the ability of different truncated versions of lincRNA-p21 to induce cellular apoptosis when overexpressed in LKR cells (Experimental Procedures). This revealed that the deletion of the 5′ end of lincRNA-p21, which mediates the hnRNP-K interaction, abolishes the ability of lincRNA-p21 to induce apoptosis (Figure 5G). Interestingly, the 780 nt fragment at the 5′ end of lincRNA-p21 alone does not induce apoptosis, indicating that this fragment is required but not sufficient for lincRNA-p21-mediated cellular apoptosis.

We hypothesized that hnRNP-K is required for proper transcriptional repression of target genes shared between p53 and lincRNA-p21. If so, knockdown of hnRNP-K should result in derepression of these shared targets. We tested this hypothesis by performing siRNA-mediated knockdown of hnRNP-K, lincRNA-p21, and p53 in p53-restored $p53^{LSL/LSL}$ MEFs, treating the cells with dox and profiling the changes in gene expression by microarray analysis.

Consistent with our previous data, we observed a strong overlap of 582 genes affected in the hnRNP-K, lincRNA-p21, and p53 knockdowns (FDR < 0.05) (Figure 6 and Figure S6). Remarkably, 83% of these common genes were derepressed in all three knockdown experiments (Figure 6A and Figure S6D). The genes previously identified as coregulated by lincRNA-p21 and p53 also were strongly enriched (GSEA FDR < 10^{-4}) among those regulated by hnRNP-K (Figure 6B and Table S3). Thus, lincRNA-p21 and hnRNP-K play roles in repressing a significant common set of genes in the p53-dependent response to DNA damage.

We further reasoned that if hnRNP-K is involved in the repression of genes corepressed by p53 and lincRNA-p21, then hnRNP-K might also be physically bound to the promoters of these genes. To test this, we performed ChIP experiments with antibodies against hnRNP-K, followed by hybridization to DNA tiling microarrays covering 30,000 gene promoters. We identified 1621 promoter regions with significant occupancy by hnRNP-K (FDR < 0.05) (Figure 6 and Table S3). Notably, these promoter regions exhibit a significant overlap with genes that were differentially expressed upon hnRNP-K knockdown (GSEA FDR < 0.001) (Figure S6E). Moreover, hnRNP-K localizes to a significant fraction (FDR < 0.001) of the genes corepressed by lincRNA-p21 and p53 (Figure 6C), suggesting that these are primary sites of hnRNP-K regulation.

We next wanted to determine whether lincRNA-p21 plays a role in hnRNP-K localization at promoters of p53-repressed genes. To this end, we determined whether siRNA-mediated knockdown of lincRNA-p21 affected the localization of hnRNP-K after induction of p53. Specifically, we performed hnRNP-K ChIP in dox-treated p53-restored $p53^{LSL/LSL}$ MEFs transfected with either siRNAs targeting lincRNA-p21 or nontargeting control siRNAs. These experiments revealed that the depletion of lincRNA-p21 causes a significant reduction in the association of hnRNP-K at the promoter regions of genes that are normally repressed in a lincRNA-p21- and p53-dependent fashion, as determined by ChIP-qPCR (Figure 6D). Specifically, 12 of the 15 tested promoter regions exhibited loss of hnRNP-K enrichment, in two biological replicate experiments, upon depletion of lincRNA-p21. Thus, hnRNP-K is bound to the promoters of genes that are normally repressed in a p53- and lincRNA-p21-dependent manner, and this localization requires lincRNA-p21.

Collectively, our results indicate that lincRNA-p21 is a direct p53 transcriptional target in response to DNA damage, acts to repress genes that are downregulated as part of the canonical p53 transcriptional response, is necessary for p53 dependent apoptotic responses to DNA damage in our cell-based systems, and functions at least in part through interaction with hnRNP-K by modulating hnRNP-K localization.

DISCUSSION

It is clear that mammalian genomes encode numerous large noncoding RNAs (Carninci, 2008; Guttman et al., 2009; Mattick, 2009; Ponjavic et al., 2007). Here, we demonstrate that numerous lincRNAs are key constituents in the p53-dependent transcriptional pathway. Moreover, we observed that some of these lincRNAs are bound by p53 in their promoter regions and sufficient to drive p53-dependent reporter activity that requires

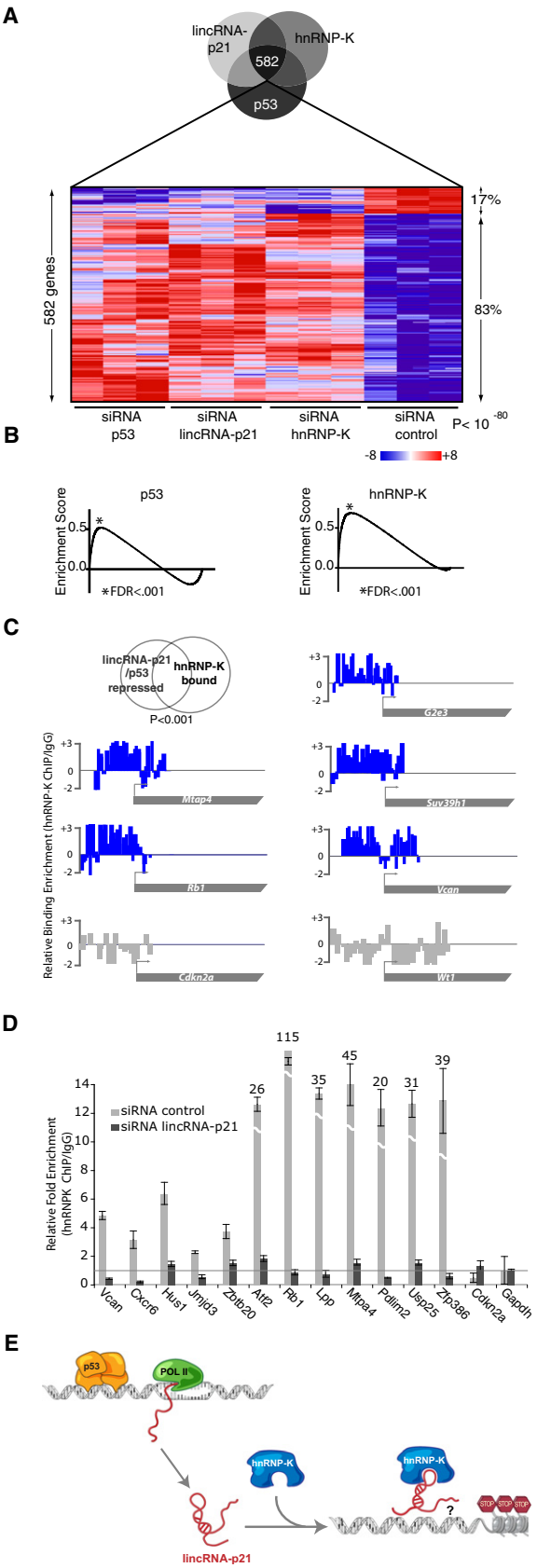

Figure 6. LincRNA-p21 and hnRNP-K Corepress Genes in the p53 Transcriptional Response

(A) Many genes are coregulated by p53, lincRNA-p21, and hnRNP-K. Genes affected by knockdown of lincRNA-p21, p53, or hnRNP-K in p53-restored-DNA-damaged $p53^{LSL/LSL}$ MEFs determined by microarray analysis (FDR < 0.05). Shades of red or blue represent expression values relative to global median across experiments. Percentages of up- and downregulated genes are indicated.

(B) Genes repressed by lincRNA-p21 are significantly enriched in genes repressed by p53 and hnRNPK. GSEA comparing the genes upregulated on knockdown of LincRNA-p21 and those upregulated upon knockdown of p53 (left) or hnRNP-K (right). The black line represents the observed enrichment score profile of genes in the lincRNA-p21 gene set to the p53 or hnRNP-K gene sets, respectively.

(C) hnRNP-K associates to promoters of genes corepressed by lincRNA-p21 and p53. Examples of promoters of genes repressed by p53 and lincRNA-p21 (G2e3, Mtap4, Suv39h1, and Vcan) or repressed by lincRNA-p21 but not p53 (Rb1) bound by hnRNP-K (blue) determined by ChIP-chip of hnRNP-K in dox-trated p53-reconstituted $p53^{LSL/LSL}$ MEFs (FDR < 0.05). Cdkn2a and Wt1 are negative controls (gray).

(D) hnRNP-K binding to lincRNA-p21 and p53 corepressed genes is dependent on lincRNA-p21. Relative enrichment of hnRNP-K (ChIP-qPCR) in the indicated promoter regions in p53-reconstituted $p53^{LSL/LSL}$ MEFs transfected with siRNA lincRNA-p21 or siRNA control and dox-treated determined by ChIP-qPCR (representative of two biological replicates shown ±STD).

(E) Proposed models for the function of licRNA-p21 in the p53 transcriptional response. Induction of p53 activates the transcription of lincRNA-p21 by binding to its promoter (upper left). LincRNA-p21 binds to hnRNP-K, and this interaction imparts specificity to genes repressed by p53 induction (upper right). See also Figure S6 and Table S3.

the consensus p53-binding motif, suggesting that these lincRNAs are bona fide p53 transcriptional targets.

Having discovered multiple lincRNAs in the p53 pathway, we decided to focus on one such lincRNA in particular: lincRNA-p21. Intrigued by its properties (genomic location upstream of *p21*, p53-dependent activation requiring the consensus p53 motif, which is bound by p53 and conserved p53-dependent activation of this gene in both human and mouse cell-based systems), we explored the functional roles of lincRNA-p21. Our studies revealed a role for lincRNA-p21 in a p53-dependent apoptotic response after DNA damage.

We further observed that siRNA-mediated inhibition of lincRNA-p21 affects the expression of hundreds of gene targets that are enriched for genes normally repressed by p53 in both the MEF and RAS cell-based systems. Strikingly, the vast majority of these common target genes are derepressed upon inhibition of either p53 or lincRNA-p21—suggesting that lincRNA-p21 functions as a downstream repressor in the p53 transcriptional response.

We gained mechanistic clues into how lincRNA-p21 functions to repress such a large subset of the p53 transcriptional response by biochemical experiments that identified a specific interaction between lincRNA-p21 and hnRNP-K. This interaction is supported by RNA-pulldown, native RIP, crosslinked RIP, and deletion-mapping experiments. Moreover, we identified a 780 nt 5′ region of lincRNA-p21 that is required for hnRNP-K binding and subsequent induction of apoptosis. Interestingly, this region is much more highly conserved than the remainder of the transcript. This suggests that patches of conservations, previously determined to be unique to lincRNAs, (Guttman et al., 2009), may point to functional elements for binding interactions within

lincRNAs (as was also recently determined for Xist binding to PRC2) (Zhao et al., 2008).

hnRNP-K is known to interact with other repressive complexes such as the Histone H1.2 or members of the Polycomb-group (PcG) (Kim et al., 2008; Denisenko and Bomsztyk, 1997). The physical interaction between lincRNA-p21 and hnRNP-K is likely required for lincRNA-p21-mediated gene repression, as loss of hnRNP-K function results in the derepression of the same genes that are repressed by both p53 and lincRNA-p21. Importantly, genome-wide ChIP-chip analysis revealed hnRNP-K binding at the promoters of these corepressed gene loci, suggestive of direct regulation by hnRNP-K and lincRNA-p21. Moreover, we observed a lincRNA-p21 dependent binding of hnRNP-K at several of these corepressed promoter regions. While hnRNP-K has been previously shown to activate one gene in the p53 pathway (Moumen et al., 2005), our analyses suggest that it plays a much more widespread role in repression. Together, these results implicate lincRNA-p21 as an important repressor in the p53 pathway, by interacting with and modulating the localization of hnRNP-K.

Our results raise the possibility that many transcriptional programs (beyond the p53-pathway) may involve inducing protein factors that activate specific sets of downstream genes and lincRNAs that repress previously active sets of genes. The notion of a noncoding RNA being involved in silencing-specific gene loci is consistent with our recent observation that many lincRNAs (including lincRNA-p21) bind to chromatin complexes (such as PRC2) and are required to mediate repression at key gene loci (Khalil et al., 2009). Moreover, there are several examples of lincRNAs involved in repression of known target genes—including HOTAIR-dependent repression of *HOXD* genes (Rinn et al., 2007) and XIST, AIR, and KCNQ1OT1, involved in genomic imprinting and silencing of several genes in *cis* (Nagano et al., 2008; Pandey et al., 2008; Zhao et al., 2008).

The precise mechanism by which lincRNA-p21 contributes to repression at specific loci remains to be defined. Various possibilities include that (1) lincRNA-p21 might direct a protein complex to specific loci by Crick-Watson base pairing; (2) lincRNAs might act by forming DNA-DNA-RNA triple-helical structures, which do not require Crick-Watson base-pairing, such as reported for a large noncoding RNA that forms a triple-helix upstream of the *Dihydrofolate Reductase* (*DHFR*) promoter resulting in repression of *DHFR* (Martianov et al., 2007); or (3) lincRNAs might alter the binding specificity of DNA-binding proteins (such as hnRNP-K) to influence their target preference (Figure 6D). Further experiments are needed to distinguish between these and other possibilities.

Aside from the general interest in gene regulation, we note that lincRNA-p21 and several other lincRNAs function in an important pathway for cancer. It is tempting to speculate that other lincRNAs may also play key roles in numerous other tumor-suppressor and oncogenic pathways, representing a hitherto unknown paradigm in cellular transformation and metastasis. It will be important for future studies to determine whether lincRNAs genes can serve as tumor suppressor genes or oncogenes.

In summary, lincRNAs may point to new mechanisms of gene regulation, components in disease pathways and potential targets for the development of therapies.

EXPERIMENTAL PROCEDURES

Cell Lines and In Vivo Models

KRAS lung tumor-derived cell lines were isolated from individual tumors (D.F. and T.J., unpublished data). Isolation of matched $p53^{+/+}$ and $p53^{-/-}$ MEFs, $p53^{LSL/LSL}$ MEFs, lymphomas, and sarcomas, and p53 restoration were done as described (Ventura et al., 2007). Primary WT MEFs and NIH/3T3 MEF cells were purchased from ATCC. Transfection, infection, and treatment conditions are described in the Extended Experimental Procedures.

Promoter Reporter Assays

LincRNA promoters were cloned into pGL3-basic vector (Promega), and motif deletions were performed by mutagenesis. p53-reconstituted or control $p53^{LSL/LSL}$ MEFs were transfected with 800 ng pGL3 and 30 ng TK-Renilla plasmid per 24-well. Twenty-four hours later, cells were treated with 500 nM dox for 13 hr, and cell extracts were assayed for firefly and renilla luciferase activities (Promega E1910).

LincRNA and Gene-Expression Profiling and Informatic Analyses

RNA isolation, lincRNA expression profiling, and ChIP-chip analyses (Nimblegen arrays), as well as Affymetrix gene-expression profiling and analyses, were performed as described (Guttman et al., 2009) (Extended Experimental Procedures). Structure predictions were performed using the Vienna RNA package (Hofacker, 2003).

Antibodies

The following antibodies were used: anti-p53, Novocastra (NCL-p53-CM5p) (western blot) and Vector Labs (CM-5) (ChIP); anti-hnRNP-K, Santa Cruz Biotechnology (sc-25373) (western blot) and Abcam (Ab70492 and Ab39975) (ChIP and RIP); and control rabbit IgG Abcam (Ab37415-5) (RIP and ChIP-chip).

Viability and Apoptosis Assays and Cell-Cycle Analysis

MTT assays were performed with Cell Proliferation Kit I from Roche (11465007001). For apoptosis quantification, the Apoptosis Detection Kit I from BD Biosciences (cat#559763) and FACS (van Engeland et al., 1996) were used. Cell-cycle analysis was performed as described (Brugarolas et al., 1995).

Cloning, RNA Pulldown, Deletion Mapping, RIP, and ChIP

5′ and 3′ RACE cloning of lincRNA-p21 were performed from total RNA of dox-treated MEFs with RLM-RACE Kit (Ambion). RNA pulldown and deletion mapping were performed as described (Rinn et al., 2007) with 1 mg mESC nuclear extract and 50 pmol of biotinylated RNA. Mass spectrometry was performed as described (Shevchenko et al., 1996). Native RIP was carried out as described (Rinn et al., 2007). For crosslinked RIP, cells were crosslinked with 1% formaldehyde, antibody incubated overnight, recovered with protein G Dynabeads, and washed with RIPA buffer. After reverse crosslink, RNA was analyzed by qRT-PCR. p53 ChIP and hnRNP-K ChIP experiments were performed as previously described (Rinn et al., 2007) (Extended Experimental Procedures).

RNA Interference and LincRNA-p21 Overexpression

siRNA transfections were done with 75 nM siRNA and Lipofectamine 2000 (Invitrogen). For overexpression, lincRNA-p21 or truncated forms were cloned into the pBABE vector. After transfection, cells were selected with 2 μg/ml puromycin.

ACCESSION NUMBERS

The accession number for the full-length mouse lincRNA-p21 sequence reported in this paper is HM210889 (bankit1350506). All primary data are available at the Gene Expression Omnibus (GSE21761).

SUPPLEMENTAL INFORMATION

Supplemental Information includes Extended Experimental Procedures, six figures, and four tables and can be found with this article online at doi:10.1016/j.cell.2010.06.040.

ACKNOWLEDGMENTS

We would like to thank Loyal A. Goff (Massachusetts Institute of Technology [MIT]) for bioinformatic support, Nadya Dimitrova (MIT) for input on the manuscript, David Garcia (MIT) for experimental assistance, and Sigrid Hart (Broad Institute) for illustration support. J.L.R. is a Damon Runyon-Rachleff, Searle, and Smith Family Foundation Scholar. J.L.R. and A.R. are Richard Merkin Foundation Scholars. This work was supported by the National Institutes of Health (NIH) Director's New Innovator Award, Smith Family Foundation, Damon Runyon Cancer Foundation, Searle Scholar Program, and NIH 1R01CA119176-01.

Received: October 6, 2009
Revised: April 6, 2010
Accepted: June 3, 2010
Published online: July 29, 2010

REFERENCES

Brugarolas, J., Chandrasekaran, C., Gordon, J.I., Beach, D., Jacks, T., and Hannon, G.J. (1995). Radiation-induced cell cycle arrest compromised by p21 deficiency. Nature *377*, 552–557.

Carninci, P. (2008). Non-coding RNA transcription: turning on neighbours. Nat. Cell Biol. *10*, 1023–1024.

Denisenko, O.N., and Bomsztyk, K. (1997). The product of the murine homolog of the Drosophila extra sex combs gene displays transcriptional repressor activity. Mol. Cell. Biol. *17*, 4707–4717.

el-Deiry, W.S., Kern, S.E., Pietenpol, J.A., Kinzler, K.W., and Vogelstein, B. (1992). Definition of a consensus binding site for p53. Nat. Genet. *1*, 45–49.

Funk, W.D., Pak, D.T., Karas, R.H., Wright, W.E., and Shay, J.W. (1992). A transcriptionally active DNA-binding site for human p53 protein complexes. Mol. Cell. Biol. *12*, 2866–2871.

Garber, M., Guttman, M., Clamp, M., Zody, M.C., Friedman, N., and Xie, X. (2009). Identifying novel constrained elements by exploiting biased substitution patterns. Bioinformatics *25*, i54–i62.

Guttman, M., Amit, I., Garber, M., French, C., Lin, M.F., Feldser, D., Huarte, M., Zuk, O., Carey, B.W., Cassady, J.P., et al. (2009). Chromatin signature reveals over a thousand highly conserved large non-coding RNAs in mammals. Nature *458*, 223–227.

Hofacker, I.L. (2003). Vienna RNA secondary structure server. Nucleic Acids Res. *31*, 3429–3431.

Khalil, A.M., Guttman, M., Huarte, M., Garber, M., Raj, A., Rivea Morales, D., Thomas, K., Presser, A., Bernstein, B.E., van Oudenaarden, A., et al. (2009). Many human large intergenic noncoding RNAs associate with chromatin-modifying complexes and affect gene expression. Proc. Natl. Acad. Sci. USA *106*, 11667–11672.

Kim, K., Choi, J., Heo, K., Kim, H., Levens, D., Kohno, K., Johnson, E.M., Brock, H.W., and An, W. (2008). Isolation and characterization of a novel H1.2 complex that acts as a repressor of p53-mediated transcription. J. Biol. Chem. *283*, 9113–9126.

Kuerbitz, S.J., Plunkett, B.S., Walsh, W.V., and Kastan, M.B. (1992). Wild-type p53 is a cell cycle checkpoint determinant following irradiation. Proc. Natl. Acad. Sci. USA *89*, 7491–7495.

Levine, A.J., Hu, W., and Feng, Z. (2006). The P53 pathway: what questions remain to be explored? Cell Death Differ. *13*, 1027–1036.

Martianov, I., Ramadass, A., Serra Barros, A., Chow, N., and Akoulitchev, A. (2007). Repression of the human dihydrofolate reductase gene by a non-coding interfering transcript. Nature *445*, 666–670.

Mattick, J.S. (2009). The genetic signatures of noncoding RNAs. PLoS Genet. *5*, e1000459.

Mercer, T.R., Dinger, M.E., and Mattick, J.S. (2009). Long non-coding RNAs: insights into functions. Nat. Rev. Genet. *10*, 155–159.

Mikkelsen, T.S., Ku, M., Jaffe, D.B., Issac, B., Lieberman, E., Giannoukos, G., Alvarez, P., Brockman, W., Kim, T.K., Koche, R.P., et al. (2007). Genome-wide maps of chromatin state in pluripotent and lineage-committed cells. Nature *448*, 553–560.

Moumen, A., Masterson, P., O'Connor, M.J., and Jackson, S.P. (2005). hnRNP K: an HDM2 target and transcriptional coactivator of p53 in response to DNA damage. Cell *123*, 1065–1078.

Nagano, T., Mitchell, J.A., Sanz, L.A., Pauler, F.M., Ferguson-Smith, A.C., Feil, R., and Fraser, P. (2008). The Air noncoding RNA epigenetically silences transcription by targeting G9a to chromatin. Science *322*, 1717–1720.

Pandey, R.R., Mondal, T., Mohammad, F., Enroth, S., Redrup, L., Komorowski, J., Nagano, T., Mancini-Dinardo, D., and Kanduri, C. (2008). Kcnq1ot1 antisense noncoding RNA mediates lineage-specific transcriptional silencing through chromatin-level regulation. Mol. Cell *32*, 232–246.

Ponjavic, J., Ponting, C.P., and Lunter, G. (2007). Functionality or transcriptional noise? Evidence for selection within long noncoding RNAs. Genome Res. *17*, 556–565.

Ponting, C.P., Oliver, P.L., and Reik, W. (2009). Evolution and functions of long noncoding RNAs. Cell *136*, 629–641.

Riley, T., Sontag, E., Chen, P., and Levine, A. (2008). Transcriptional control of human p53-regulated genes. Nat. Rev. Mol. Cell Biol. *9*, 402–412.

Rinn, J.L., Kertesz, M., Wang, J.K., Squazzo, S.L., Xu, X., Brugmann, S.A., Goodnough, L.H., Helms, J.A., Farnham, P.J., Segal, E., and Chang, H.Y. (2007). Functional demarcation of active and silent chromatin domains in human HOX loci by noncoding RNAs. Cell *129*, 1311–1323.

Schaefer, B.C. (1995). Revolutions in rapid amplification of cDNA ends: new strategies for polymerase chain reaction cloning of full-length cDNA ends. Anal. Biochem. *227*, 255–273.

Shevchenko, A., Wilm, M., Vorm, O., Jensen, O.N., Podtelejnikov, A.V., Neubauer, G., Shevchenko, A., Mortensen, P., and Mann, M. (1996). A strategy for identifying gel-separated proteins in sequence databases by MS alone. Biochem. Soc. Trans. *24*, 893–896.

Subramanian, A., Tamayo, P., Mootha, V.K., Mukherjee, S., Ebert, B.L., Gillette, M.A., Paulovich, A., Pomeroy, S.L., Golub, T.R., Lander, E.S., and Mesirov, J.P. (2005). Gene set enrichment analysis: a knowledge-based approach for interpreting genome-wide expression profiles. Proc. Natl. Acad. Sci. USA *102*, 15545–15550.

Ule, J., Jensen, K., Mele, A., and Darnell, R.B. (2005). CLIP: a method for identifying protein-RNA interaction sites in living cells. Methods *37*, 376–386.

van Engeland, M., Ramaekers, F.C., Schutte, B., and Reutelingsperger, C.P. (1996). A novel assay to measure loss of plasma membrane asymmetry during apoptosis of adherent cells in culture. Cytometry *24*, 131–139.

Vazquez, A., Bond, E.E., Levine, A.J., and Bond, G.L. (2008). The genetics of the p53 pathway, apoptosis and cancer therapy. Nat. Rev. Drug Discov. *7*, 979–987.

Ventura, A., Kirsch, D.G., McLaughlin, M.E., Tuveson, D.A., Grimm, J., Lintault, L., Newman, J., Reczek, E.E., Weissleder, R., and Jacks, T. (2007). Restoration of p53 function leads to tumour regression in vivo. Nature *445*, 661–665.

Wei, C.L., Wu, Q., Vega, V.B., Chiu, K.P., Ng, P., Zhang, T., Shahab, A., Yong, H.C., Fu, Y., Weng, Z., et al. (2006). A global map of p53 transcription-factor binding sites in the human genome. Cell *124*, 207–219.

Zhao, J., Sun, B.K., Erwin, J.A., Song, J.J., and Lee, J.T. (2008). Polycomb proteins targeted by a short repeat RNA to the mouse X chromosome. Science *322*, 750–756.

Cell

EXTENDED EXPERIMENTAL PROCEDURES

Cell Lines, p53 Restoration and DNA Damage Induction

Lung tumor-derived cell lines were isolated from individual tumors from *KrasLA2/+; Trp53LSL/LSL Rosa26CreERT2* animals (D.F. and T.J., unpublished data). Lymphomas and Sarcomas were isolated when they formed in *Trp53LSL/LSL Rosa26CreERT2* animals as described (Ventura et al., 2007). For p53 restoration, cultured tumor cell lines were incubated with 500nM 4-hydroxytamoxifen (Sigma) for the indicated time points and $p53^{LSL/LSL}$ MEFs, were infected with AdenoCre virus or AdenoGFP for 24h (University of Iowa) at moi of 5. For DNA damage, cells were treated with 100 to 500nM doxorubicin hydrochloride (Sigma D1515).

RNA Purification and qRT-PCR Analysis

Total RNA from cells was isolated using Trizol reagent (Invitrogen) and purified with RNeasy kit (QIAGEN) following manufacturers instructions. Reverse Transcription was performed using High Capacity cDNA Reverse Transcription Kit (Applied Biosystems) and real time PCR was performed with SYBR green master mix (Roche). Gapdh RNA levels were used for normalization.

qPCR Primers

qRT-PCR and ChIP-qPCR primer sequences are listed in Table S4.

LincRNA and Protein Coding Gene Expression Profiling

High resolution DNA tiling arrays were designed on the Nimblegen platform to represent a random sampling of ~400 lincRNAs identified in the mouse genome. Total RNA from different experimental conditions was amplified using poly-dT and labeled as described (Guttman et al., 2009).

Identifying Differentially Expressed lincRNAs

We designed custom Nimbelgen tiling microarrys which tile the exonic regions of each mouse lincRNA at 10bp resolution. To identify lincRNAs that were differentially expressed in these conditions, we first determined which lincRNAs are significantly expressed in each sample. We then used this set of expressed lincRNAs to test for differential expression.

To determine expressed lincRNAs we used our previously developed statistical algorithm to identify peaks in hybridization. We first normalized the data by dividing each probe value by the average probe intensity across the array. We scanned each region and computed a score defined as the sum of the normalized probe intensities. To determine the significance of this score we permuted the intensity values assigned to each probe and recalculated the statistic. We took the value for each permutation as the maximum score obtained for any random region. We performed 1000 permutations and assigned a multiple testing corrected p-value to each region based on its rank within this distribution. All exons with a p-value less than 0.05 were retained.

We computed differentially expressed exons by extending the above strategy but computed a t-statistic between each group (ie 0hr versus 8hr). We assessed a multiple testing corrected p-value by permuting the probe values across all conditions and recomputing the t-statistic. We performed 1000 permutations and generated a maximum distribution for each permutation and assigned FWER corrected p-values. We retained all exons with p-values < 0.05.

We performed post-processing of these results to ensure robust differential lincRNAs. Specifically, for MEF time course we required that a lincRNA exon was differentially expressed between $P53^{+/+}$ and $P53^{-/-}$ cells and also differentially expressed between any time point and time 0. For the KRAS experiment we required that any differential exon be differentially expressed in 2 consecutive time points compared to time 0.

p53 Chromatin Immunoprecipitation

$p53^{+/+}$ or $p53^{-/-}$ MEFs were treated with 0.2 mM/ml doxorubicin for 6 hr, crosslinked with Formaldehyde (10 min at 1%), harvested and washed once with Farnham lysis buffer (5 mM PIPES pH 8.0, 85 mM KCl, 0.5% NP-40, supplemented with Roche protease inhibitor cocktail). The nuclear pellet was resuspended in RIPA buffer (1 x PBS, 1% NP-40, 0.5% Na-deoxycholate, 0.1% SDS supplemented with Roche protease inhibitor cocktail) and sonicated. Antibodies were coupled to PBS/BSA (5mg/ml) blocked Dynabeads overnight. After overnight incubation of the sonicated chromatin with the antibody-coupled beads, the beads were washed 5 x with LiCl wash buffer (100 mM Tris pH 7.5, 500 mM LiCl, 1% NP-40, 1% Na-deoxycholate) and 1 x with TE (10 mM Tris pH 7.5, 0.1 mM Na_2EDTA). The ChIPed DNA was eluted for 1 hr at 65°C in Elution buffer (1% SDS, 0.1 M $NaHCO_3$), reverse X-linked, purified and analyzed by qPCR.

Protein Coding Gene Expression Profiles

We generated expression profiles for protein coding gene expression using Affymetrix 430 2.0 arrays. We identified differentially expressed genes using the Patterns from Gene Expression (http://www.cbil.upenn.edu/PaGE/) program. Briefly, we determined differential expression using a t-statistic between groups and permutation distribution to compute an FDR for each gene. We filtered all genes with an FDR < 0.05 as significantly differentially expressed. We filtered the list by genes similar to the criteria used for the lincRNA (tiling arrays). We required differential expression between $P53^{+/+}$ and $P53^{-/-}$ for each time point and differential expression compared to time 0. For the RAS experiment we required differential expression of each gene for at least 2 consecutive time points.

Gene Set Enrichment Analysis and Functional Term Clustering

Gene Set Enrichment Analysis was performed as previously described (Grant et al., 2005, Subramanian et al., 2005). Briefly, we used each condition as a group (ie siLincRNA-p21 versus siControl) and ranked the gene list based on differential expression between the groups. The rank of these genes was used to identify significant gene sets, using the weighted Kolmogorov–Smirnov (KS) test (Grant et al., 2005). Gene sets were permuted 1000 times to obtain FDR corrected p-values. We used gene sets representing the Molecular Signatures Database or custom gene sets defined by other experiments.

Chromatin Map Data

Chromatin data for H3K4me3 and H3K36me3 for mouse embryonic stem cells (mESCs) mouse were taken from Mikkelsen et al., 2007 and were downloaded from (ftp://ftp.broad.mit.edu/pub/papers/chipseq/).

p53 Motif Analysis

To scan for conserved motifs in putative P53 targets we used an extension of the a method that scores conservation at single nucleotide resolution based on the evolutionary substitution pattern inferred for the site (Garber et al., 2009). Motifs were represented by Position Weight Matrix (PWM) downloaded from the TRANSFAC matrix database v8.3 (http://www.gene-regulation.com/pub/databases.html) (Garber et al., 2009). Given a PWM, for each nucleotide position in a promoter, we calculated an affinity score defined as the log likelihood (LOD score) for observing the sequence given the PWM versus a given random genomic background. We then found the best conserved motif instance over the entire promoter region for each PWM. An instance was considered conserved if its conservation score was in the top 5% of the genome distribution.

We computed this score for each lincRNA promoter and computed enrichment of the motif for our experimentally determined set compared with all lincRNA promoters. To ensure that enrichment was not due to nucleotide bias within the promoter, we shuffled the PWM and computed enrichment for the true PWM compared to the shuffled PWMs. Enrichment was computed using a two-sided Wilcoxon rank-sum test between the set and the background. We then computed an FDR to correct for testing of multiple PWMs.

RNA Interference and LincRNA-p21 Overexpression

siRNA oligos targeting lincRNA-p21 (#1 UGAAAAGAGCCGUGAGCUA, #2 AAAUAAAGAUGGUGGAAUG and #3 AGUCAAAGGC AAUGAGCAU) and hnRNP-K (siRNA smart pool M-048002) were purchased from Dharmacon. p53 siRNAs (#1 AGAAGAAA AUUUCCGCAAA and #2 ACAGCGUGGUGGUACCUUA) were purchased from Ambion. Non-targeting siRNAs were purchased from Dharmacon (D-001206-14) and Ambion (AM4636). siRNA transfections were done with 75nM of siRNA and Lipofectamine 2000 (Invitrogen) following manufacturer's instructions. For overexpression, LincRNA-p21 was cloned into the pBABE vector and after transfection cells were selected with 2mg/ml puromycin for 8 days. For gene expression profiling of lincRNA-p21 overexpression, pBABE plasmid expressing lincRNA-p21 or empty vector were transfected into p53-reconstituted $p53^{LSL/LSL}$ MEFs and 24 hr later treated with 500nM doxorubicin. 14h after treatment total RNA was extracted for microarray analysis.

Nuclear Fractionation

For nuclear fractionation 10^7 cells were harvested and resuspended in 1ml of PBS, 1ml of buffer C1 (cell lysis buffer, QIAGEN) and 3ml of water, and incubated for 15 min on ice. Then cells were centrifuged for 15 min at 2,500 rpm, the supernatant was discarded and the nuclear pellet was kept for RNA extraction.

LincRNA-p21 Sequence

Sequence of the lincRNA-p21 full length clone from doxorubicin-treated mouse embryonic fibroblast:

```
> lincRNA-p21
TGGCAGTCTGACCCACACTCCCCACGCCCAGGACCAAGTCGCCTGAGCCCCATAGCCACAACTCTCTGCCGGCCTTGCCCGGGCTTGCCTT
CGGTTGCATCATCTCCCAGCTTTGCCAGGGGTGCAGAAGTGAACCACCCACTCAGCGCTGGAAAAACCAGCTAATTATATCTCCAAAGAC
CCAGGGCAAGAACTTGTGGACAACCTCAGCTGGCCTGGCCTGTCCCACTCGCTTTCCATTTCCCCCCACCCTGAGACAGGATGCCACTGTG
TAGCCCAGTGTAGTGAACACTTGGAATACAAAATAAAGATGGTGGAATGAGACATTCCGTCTCCAGTTCCTAACATCAGAAGTGAGCACCT
GTGTGTCACCAGCAACATATTGGAGGCCAGCTGCCTACACCAATCAGAAACAGGGACCACAAAGTCTGCAGGGGTGAGATAGGCCTTTTC
AGTGTCTACGATTTCATCATGGACATTACTGTCGATTTCTCTTCCTGCCCCTGTATGTGCGGGTCTATCGCCATCTCGCCATCTCCGGCT
CCTGTGTTATGAAGACAGTCTCATGCAGCCCAGACCAATCTCAAATTGACTAGGTAAACTGAGGCTGGCCTTGAACCAGTCCCTCCTGCC
TCTATCTCCTGAGAGCTGGGTAACAGCTTCTGGAGCCTCACCCAGCTTCGCTTTCACCACCCCAGCCAATCCTGTGACTCCTCTTCATAG
CGAGAGCATTGACACTTATGTTCTGAGTGTGAAAAAAAAAAAAAAATCACATAGTACTTCCTACTAGAACCTTGCCCGGGTCAACTGAAG
TGTGTGTGTTTGCTTACCAGTCTGCAGGTTTGCTTAAGTTTGTTTATTTTAGAGACCAGGTCTTGCTCTGTTGCCTAAGCCAACTTGAAAC
TCTTGGGCTCCAACAGTTCTCCTGCTCCATCTTTCTAGAGCAGCTGGGACTCTAGGCATGCTCCACTACAGCTGACTGAAGCTTGAATGAA
TGAATGAATGAATGAATGAGTTACTACCTCTGAGGGACCCTCCTCATGGCCTTCTCAACTCTGTACTTTAATTAGTTGCTTAGAGGTGTCT
CCATGCCTCAGTTTCCCCATCTGTAATAGTAAACGAGTTCACAGGCGTGGTCTGTGCTTGGAGCAAGAACAAAACCATCCTGGCCTATACT
CTCTAGGGACTCTACAGAGCCCATCCCTTTGGCTATCAGACTGTTGAGATAAAGGTTCCCCCAGGAATCGGAATCCCCTCCGACAGGAGTC
TCATGCTCAGAGAAGAAAAAAAGCTGAAGCCTGCTGACAGCCAGAGAGGGTACTTGTCTGTCAGGGAAAAATTCTACACAGGACAGACTGG
```

AGCCCAGACTGGTCTGGGTCAGTGACACACGGCACAGCACACGGTGGGACAACCTGGCTGTGCATCTCTCTCAAACCTCTTGTCACCCTTC
TCACTGTGGCCACAGCGAAGCGAATACATCTCTCTGCTTTTCACTACGTAGCTCCATCATTGCCTTGGGGGGGGGTAGCGAGGAAGGTCAC
TGGGGCCCTGCCTCTGATAAGAAGAACGAGCAATTATGATTTCCAGGAACCGAGGGTGCTCTTGCTGTTCAGTGTCTCCAGCACCCCCGGA
GACCCCAGGGCTGCCGTCAAGGGTGTTCAATAAACACGTATCGATTGAGCCAACAATGCCAGAATTGGACCTGCAGAGGAGAAAATGGACA
AACAAGACAGTGAGCCTGCAGGTGAGACCAGAACTGGAGCCAACAATCTACCTCTCTCTCCCAACCCTAGCAACGCCAGCAGCTCTCTGGG
CGAGGGGCACAGTTGCTTCCAGTTGGCAGAACCAGTCTCCCAGCTTCCCTTCAGAACCCAGCACCTGCTGAGCCACCGACCCACGGACTGT
CTCTCTCTGGAAGGCAGCCACCGACCCACGGACTGTCTCTCTCTGGAAGGCAGTTCACCTCTGGGTTTCAACACTGCCCTTTCCCCTTTCC
TTCTTTAGCCCTTAGGAATCCCTGAAAGCTTCCTGTGCTTGTGGCTTCTGTGACTTCTCAACATCTCTTGTGCACACACACACACACACAC
ACACACACACACCAGCCTGTGTCTAAGCAGTTCATCCTGTACAATGTCTCTCTGATAAAATAACTGATTCCATTTCTGTCACCTGCTGAGG
CTCCAGCAGCTCTGCCCTCAGACCTCTTAAAGCTGAGGCTCAGAAGCACAGGGAGGCACGGGAACCTGGTCCCAGGCCCTGGCTTGCTGGA
GCGAAGGAATCTATTGCTTCGGCCACTCGGTCAGAATCCCTCGGAGATTGATGTGATATGCACAGTGACACCCAATCGGGCTTGGAAAACT
GGGCCAACAGTTAAGCCACACAAAGGAACTAACCACAGCTCCACTGGCAACTGGCTCCTTGGCAAGTGCCAAAACAAACAGCTGTGGTGCA
GGCCTTCCCCGGGCTGCCGGCTTCCTGGACACTGGCAGAGGCCGCTCAAGAAGGGAGTACCTGAGTAGGGTGTTGTTCAGTTGGTAGAACG
TTTGCTTGCCTTCCATGAAGCCCAGGGTTCTGTCTGCACCTCATACCTGTGATCCTAGCAGTTGGGAAAAGACAGCAAGCACCCGGATCAG
AAGTTCAAGACCACCCTCCCCTTTATAAAGGGATCTGAGGCAGCCTGGGACATCTGAATGACAAATGAAAAGAGCCGTGAGCTATCTGGTG
TTTTCTTCATGGAAGTCCAAGTCTCCCCCTCATTCCTCCCAGGATTCTCCGAATCTGGCTGTTGTCTTTTGCGATATTTTAGAATATTCTA
GCCAGAGCGCAGAGTATAAAATACAAGTCAAAGGCAATGAGCATATGTTAGATGGATGGAGGAGGGCCTAAAAATGCTGGTGCTGGGGAGG
AAAAATGGCTCAGCAGTTAAGAGCACCGGCTGCTTTTACAGAGGACCTGCCTTCAGTTCACAGCAACCGCATGACGGCAACTCTGGTTCCA
GGAAATCCAATGCCCTCTTCTGACCTCTATAGGCACCCGGCAAGCACACAGTGCACAGACAATCATACACACGTGT.

SUPPLEMENTAL REFERENCES

Garber, M., Guttman, M., Clamp, M., Zody, M.C., Friedman, N., and Xie, X. (2009). Identifying novel constrained elements by exploiting biased substitution patterns. Bioinformatics *25*, i54–i62.

Grant, G.R., Liu, J., and Stoeckert, C.J., Jr. (2005). A practical false discovery rate approach to identifying patterns of differential expression in microarray data. Bioinformatics *21*, 2684–2690.

Guttman, M., Amit, I., Garber, M., French, C., Lin, M.F., Feldser, D., Huarte, M., Zuk, O., Carey, B.W., Cassady, J.P., et al. (2009). Chromatin signature reveals over a thousand highly conserved large non-coding RNAs in mammals. Nature *458*, 223–227.

Hofacker, I.L. (2003). Vienna RNA secondary structure server. Nucleic Acids Res. *31*, 3429–3431.

Subramanian, A., Tamayo, P., Mootha, V.K., Mukherjee, S., Ebert, B.L., Gillette, M.A., Paulovich, A., Pomeroy, S.L., Golub, T.R., Lander, E.S., and Mesirov, J.P. (2005). Gene set enrichment analysis: a knowledge-based approach for interpreting genome-wide expression profiles. Proc. Natl. Acad. Sci. USA *102*, 15545–15550.

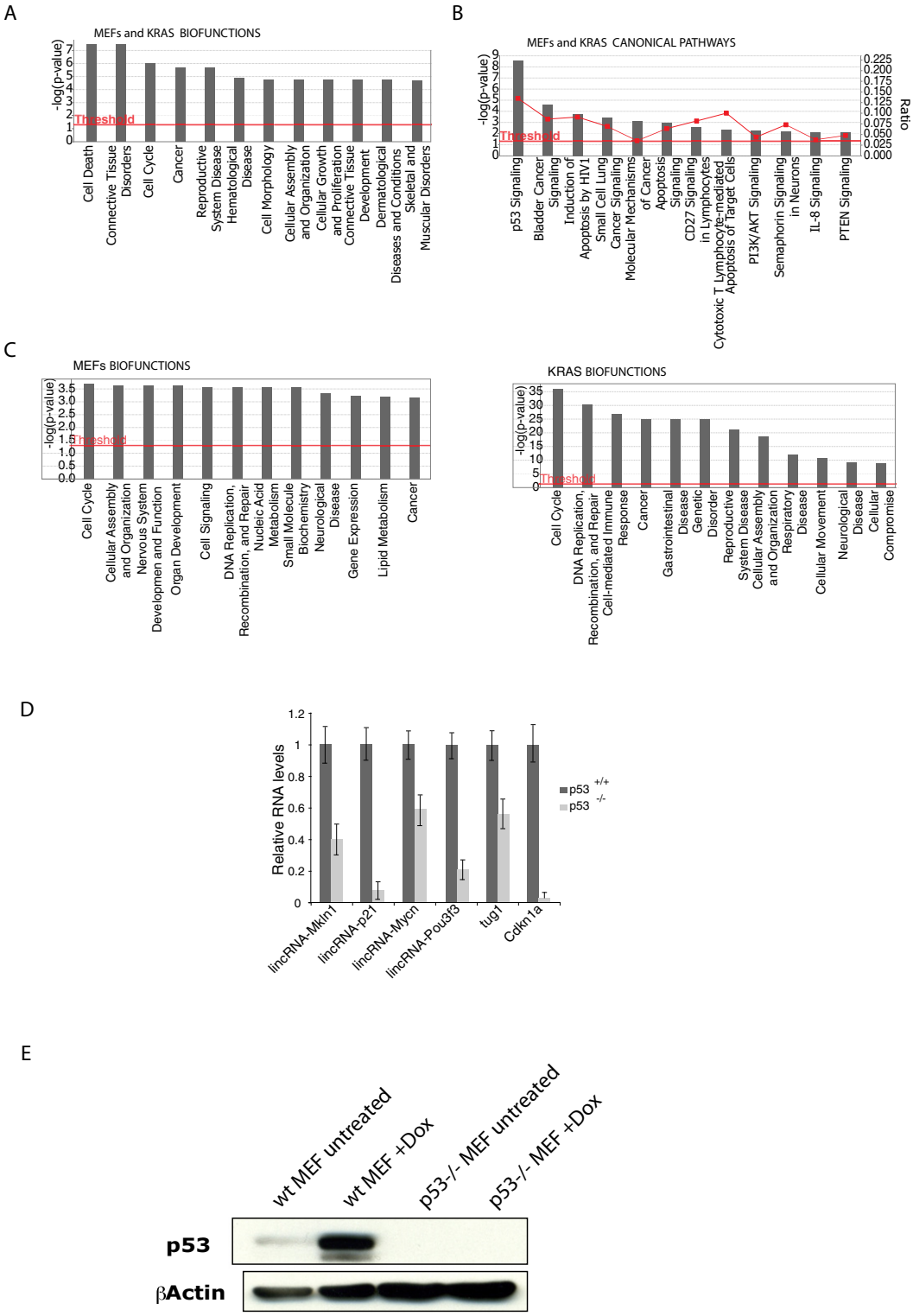

Figure S1. Protein-Coding Genes Induced in the "MEF" and "KRAS" Systems in a p53-Dependent Fashion Are Enriched in p53 Terms, Related to Figure 1

(A) Top significant biofunctions of protein-coding genes commonly upregulated in the "MEF" and "KRAS" model systems in a p53 dependent manner.
(B) Top significant canonical pathways of the genes commonly upregulated in the "MEF" and "KRAS" model systems in a p53 dependent manner.
(C) Most significant biofunctions of the protein-coding genes specifically regulated by p53 in the "MEF" but not "KRAS" experimental system (left panel) or in the

"KRAS" but not "MEF" experimental system (right panel).
Analyses were performed with Ingenuity Pathways Knowledge Base. The significance of the enrichment of each biofunction or pathway in each gene set is plotted as -log(p-value) and red lines indicate p = 0.05. Red squares represent the proportion of genes of a given pathway that are present in the experimental gene set (ratio).
(D) Relative lincRNA transcript levels in $p53^{+/+}$ (dark gray) or $p53^{-/-}$ (light gray) KRAS lung tumor cells (lincRNA-Mkln1, lincRNA-p21, lincRNA-Adamts16, lincRNA-Pou3f and lincRNA-Zf281) or MEFs (lincRNA-Actl7b, lincRNA-Mycn and tug1).
(E) WB showing the specific induction of p53 by Dox treatment in p53 wt MEFs but not p53−/− MEFs used for p53 ChIP experiment.

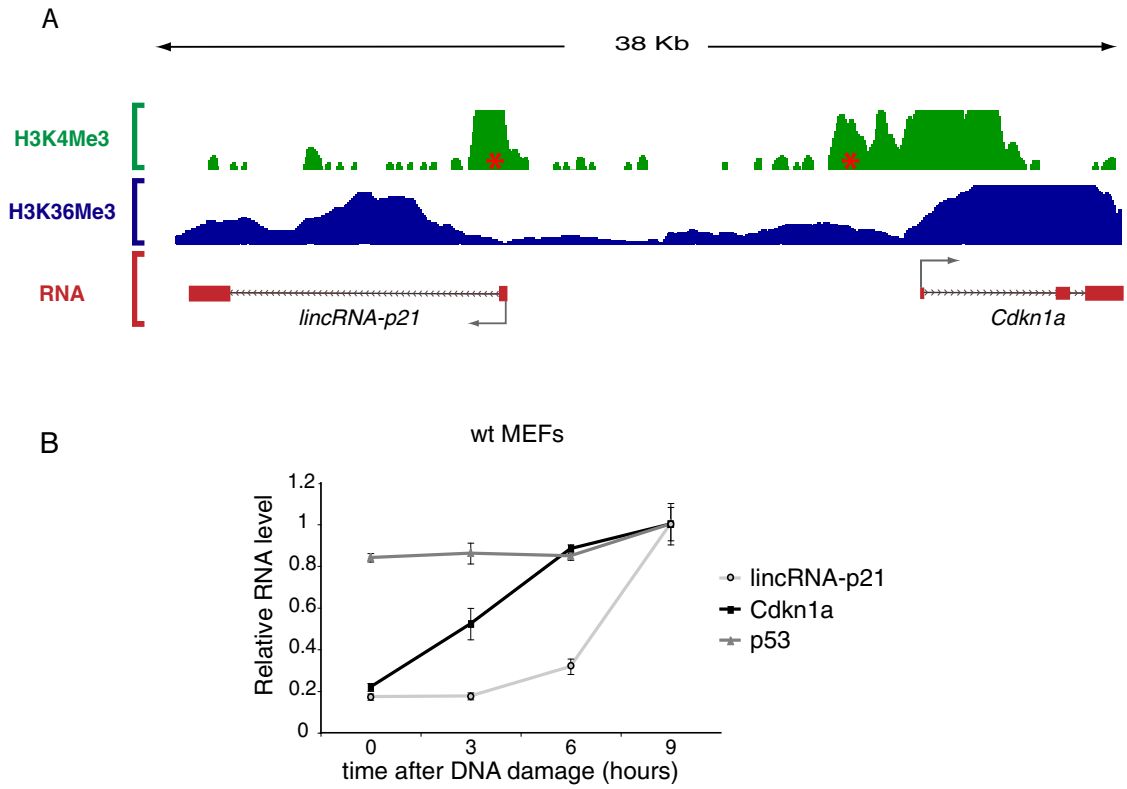

Figure S2. LincRNA-p21 and Cdkn1a Are Two Independent p53 Target Genes, Related to Figure 2

(A) Chromatin structure of lincRNA-p21 and Cdkn1a loci. The chromatin structure at the lincRNA-p21 and Cdkn1a loci is shown as mESC ChIP-Seq data; for each histone modification (H3K4me3, green; H3K36me3, blue), the results of ChIP-sequence experiments are plotted as the number of DNA fragments obtained by ChIP-sequence at each position divided by the average number across the genome. Red stars indicate the position of the p53 binding motifs in lincRNA-p21 and Cdkn1a promoters. The structures of lincRNA-p21 and Cdkn1a genes are represented with red boxes as exons and arrowed lines as intronic sequences. Grey arrows indicate the direction of transcription.

(B) Temporal induction of lincRNA-p21 and Cdkn1a in wt MEFs treated with DNA damage. MEFs were treated with 500nM doxorubicin and RNA was harvested at 0, 3, 6 and 9 hr after treatment. RNA was extracted and lincRNA-p21 (light gray), p53 (medium gray) and Cdkn1a (black) RNA levels were determined by qRT-PCR. RNA levels are the median of 4 technical replicates normalized to 9 hr +/−STD.

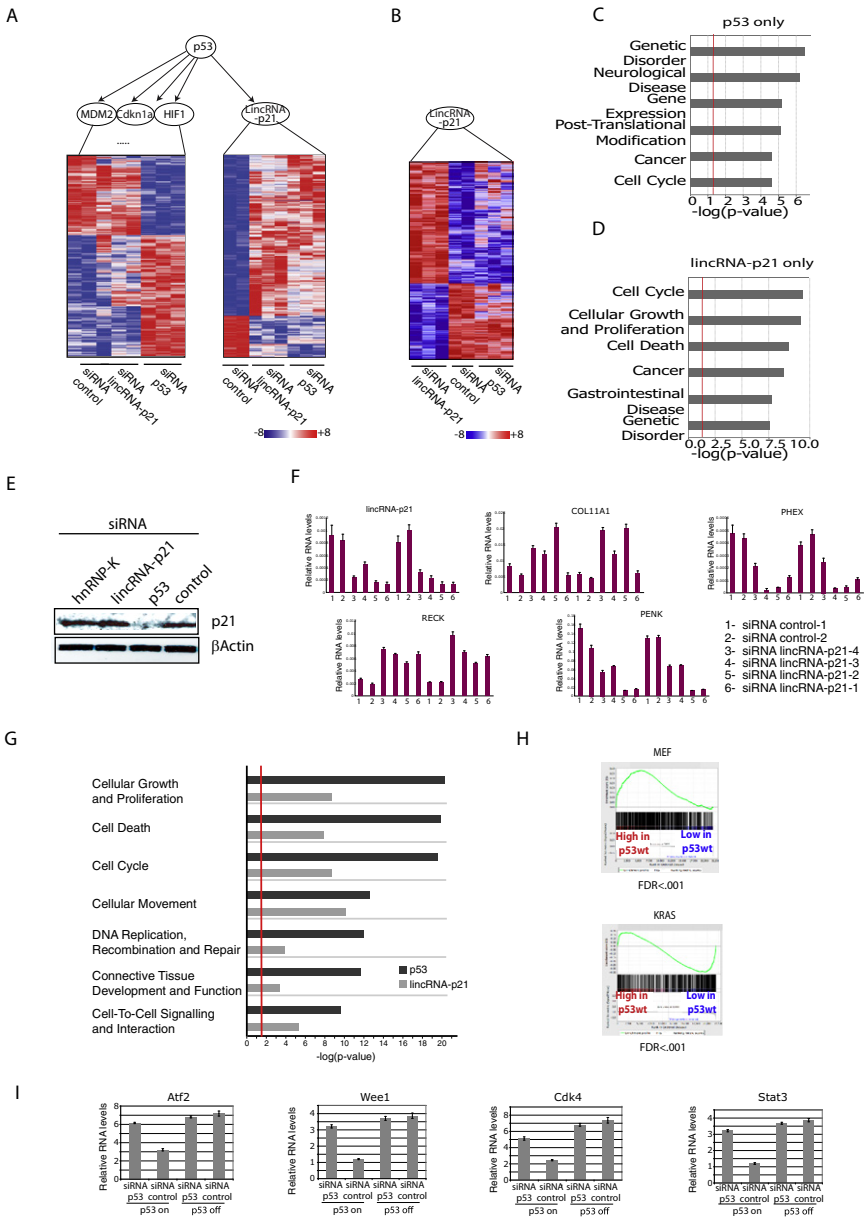

Figure S3. LincRNA-p21 Mediates Gene Repression in the p53 Pathway, Related to Figure 3

(A) Protein-coding genes affected by p53 but not lincRNA-p21 siRNA treatments (left panel) or commonly affected by lincRNA-p21 and p53 siRNA treatments (right panel) relative to siRNA control. Shades of red and blue are scaled to 8-fold activation and repression respectively.

(B) Protein-coding genes affected by lincRNA-p21 but not p53 siRNA treatments relative to siRNA control.

(C) and (D). Most significant biofunctions of genes affected by p53 but not lincRNA-p21 depletion (C) or by lincRNA-p21 depletion but not p53 depletion (D). Analyses were performed with Ingenuity Pathways Knowledge Base and the significance of the enrichment of each biofunction in each the gene set is plotted as -log (p-value) and red lines indicate p = 0.05.

(E) p21 protein levels in p53-reconstituted $p53^{LSL/LSL}$ MEFs treated with the indicated siRNAs followed by 14 hr of 100nM dox treatment. bActin levels are shown as control.

(F) qRT-PCR validation of lincRNA-p21 microarray data by lincRNA-p21 depletion with independent siRNA oligos. p53-reconstituted $p53^{LSL/LSL}$ MEFs were transfected separately with 4 different siRNAs targeting lincRNA-p21 or a siRNA control pool and treated with 100nM doxorubicin for 14 hr. The RNA was extracted and tested by qRT-PCR for lincRNA-p21 (top left), Col1A1 (top middle), Phex (top right), Reck (bottom left) and Penk1 (bottom middle) RNA levels. Each experiment was done in two biological replicates and each bar represents one biological replicate and the median of 4 technical replicates +/−STD.

(G) Genes regulated by lincRNA-p21 and p53 are enriched in terms of the p53 biological response. Plot of the gene ontology (GO) enrichment analysis (Supplemental Experimental Procedures) of the genes affected by p53 knock down (dark gray) or lincRNA-p21 knock down (light gray). The enrichment P value is plotted as -log(P value) on the *x* axis. Red line denotes p = 0.05.

(H) Genes regulated by lincRNA-p21 enforced expression significantly overlap with genes specifically regulated by p53 restoration in the MEF (upper panel) and

KRAS (lower panel) systems (FDR < .001). The green line represents the observed enrichment score profile of protein coding genes induced by lincRNA-p21 overexpression in DNA damaged-p53 reconstituted-p53$^{LSL/LSL}$ MEFs with genes regulated in a p53-dependent manner in the MEF and KRAS systems (left and right panels respectively). Enrichment was determined by Gene Set Enrichment Analysis (GSEA).

(I) Genes induced by lincRNA-p21 and p53 depletion are specifically repressed by p53. Relative RNA levels of Atf2, Wee1, Cdk4 and Stat3 genes determined by qRT-PCR in p53$^{LSL/LSL}$ MEFs where p53 allele has been reconstituted (p53 on) or not (p53 off) and treated with p53 siRNA or control siRNA. Values represent the median of 4 technical replicates +/−STD.

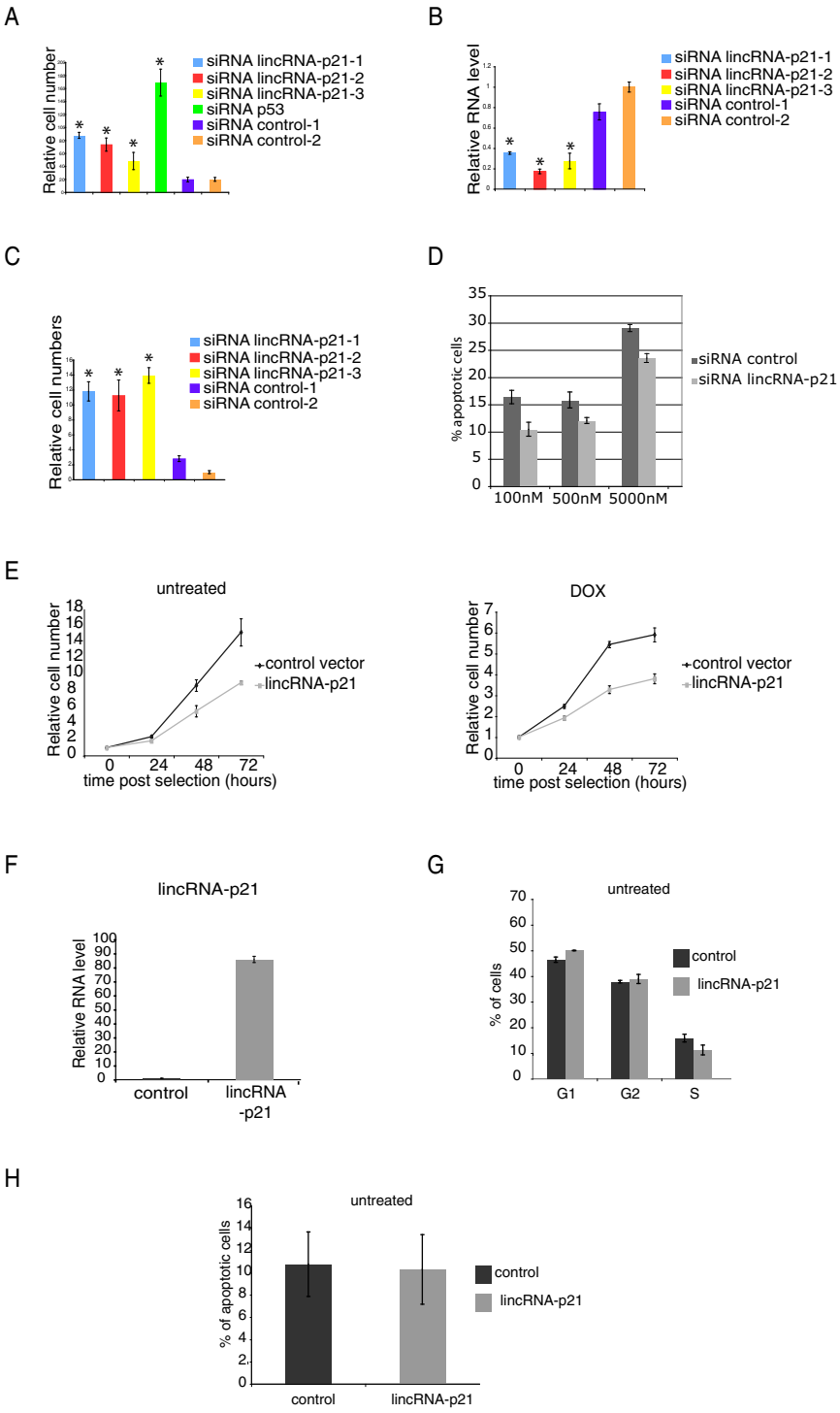

Figure S4. LincRNA-p21 Regulates Cellular Apoptosis, Related to Figure 4

(A) LincRNA-p21 depletion increases cell viability. Relative number determined by MTT assay of wild-type MEFs 96 hr after siRNA transfection with three independent lincRNA-p21 siRNAs (light blue, red and yellow), a p53 siRNA pool (green) or two independent non-targeting siRNA pools (dark blue and orange). Cells were treated with 400nM doxorubicin (DOX) from 24h after transfection. Values represent the average of three biological replicates +/−STD, and stars represent significant difference (P<0.01) to control siRNAs.

(B) LincRNA-p21 depletion by independent siRNA oligos. MEFs were transfected with three independent siRNAs targeting lincRNA-p21 or two independent non-targeting siRNA pools as control. 24 hr after transfection cells were treated with 100nM doxorubicin and 24 hr later RNA was extracted and lincRNA-p21 levels were quantified by qRT-PCR. Values represent the median of 4 technical replicates +/−STD, and stars represent significant difference (P<0.01) to control siRNAs.

(C) LincRNA-p21 depletion with independent siRNAs induces increased cell viability. MEFs were treated as in (B) and 72 hr after transfection the number of cells was determined by counting cells in 16 random live microscopy fields per condition. Values represent the average of 3 biological replicates +/−STD, and stars represent significant difference to control siRNAs.
(D) Apoptosis induction in p53-reconstituted $p53^{LSL/LSL}$ is dependent on the Dox dosage. Percentage of apoptotic cells determined by FACS analysis of Annexin-V positive cells after treatment with the indicated dosages of Dox for 14 hr. Values are average of 3 biological replicates +/−STD.
(E) Overexpression of lincRNA-p21 in 3T3 MEFs affects cell viability. 3T3 MEFs were transfected with a puromycin resistance vector expressing lincRNA-p21 (light lines) or the empty vector as control (dark lines) and after puromycin selection cells were grown in the presence (right panel) or absence (left panel) of DNA damage. At different times after platting the number of viable cells was determined by MTT assay. Each value represents the average of 3 biological replicates +/− STD.
(F) LincRNA-p21 overexpression in untreated LKR cells. Relative RNA levels of lincRNA-p21 in LKR cells transfected and selected with a plasmid overexpressing lincRNA-p21 (light bars) or a control plasmid (dark bars). Values are the median of 4 technical replicates +/−STD.
(G) LincRNA-p21 overexpression in LKR cells. Proportion of cells in the G1, G2 and S phases of cell cycle determined by BrdU and PI staining followed by FACS analysis of LKR cells overexpressing lincRNA-p21 (light bars) or a control plasmid (dark bars). Values represent the median of 3 biological replicates +/−STD.
(H) LincRNA-p21 overexpression in untreated LKR cells. Proportion of apoptotic cells determined by Annexin-V staining and FACS analysis of LKR cells overexpressing lincRNA-p21 (light bar) or control plasmid (dark bar). Values represent the median of 3 biological replicates +/−STD.

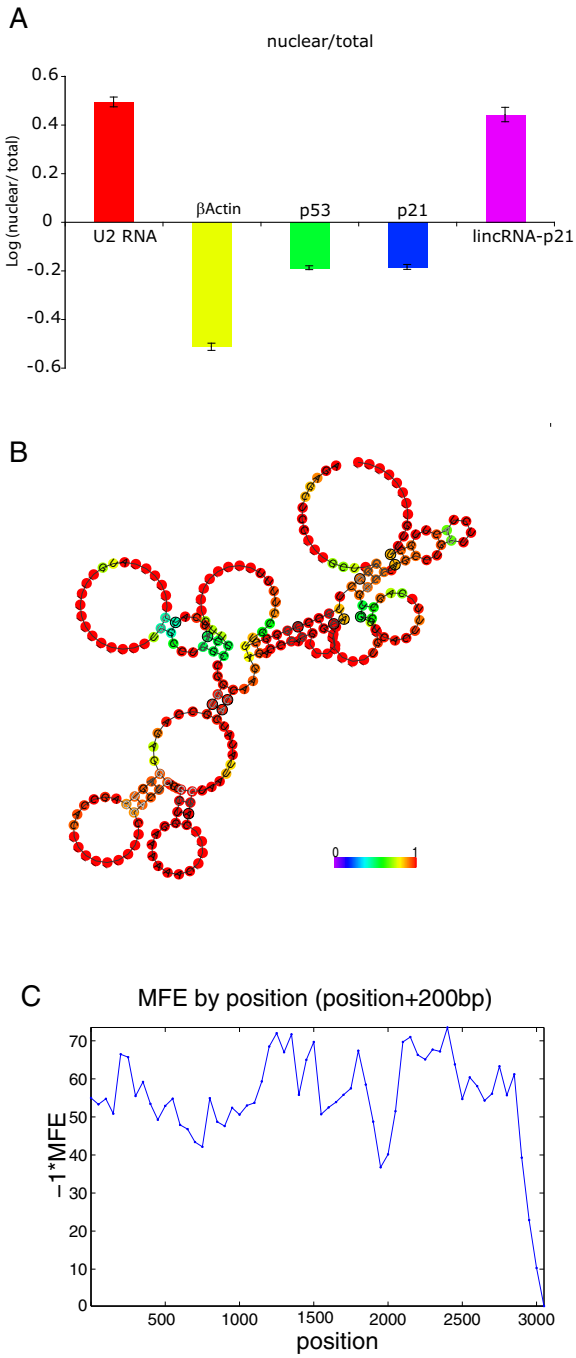

Figure S5. LincRNA-p21 Is Enriched in the Nuclear Compartment of the Cell, Related to Figure 5

(A) RNA was extracted from nuclei and cytoplasm (total) or only nuclei (nuclear) of p53-reconstituted $p53^{LSL/LSL}$-DNA damaged-MEFs. 1 μg of RNA was used for qRT-PCR analysis of lincRNA-p21, U2 RNA (nuclear retained) and p21, p53 and βActin mRNAs (exported to cytoplasm). Values represent the median of 4 technical replicates +/−STD.

(B) Prediction of lincRNA-p21 structure of a130-280nt region based on sequence conservation and compensatory mutations (Hofacker, 2003). Color scale indicates the confidence for the prediction for each base with shades of red indicating strong confidence.

(C) Negative representation of the Minimal Free Energy (MFE) (kcal/mol) associated to structures in 200nt increments of lincRNA-p21 RNA sequence determined by Vienna RNA package (Hofacker, 2003).

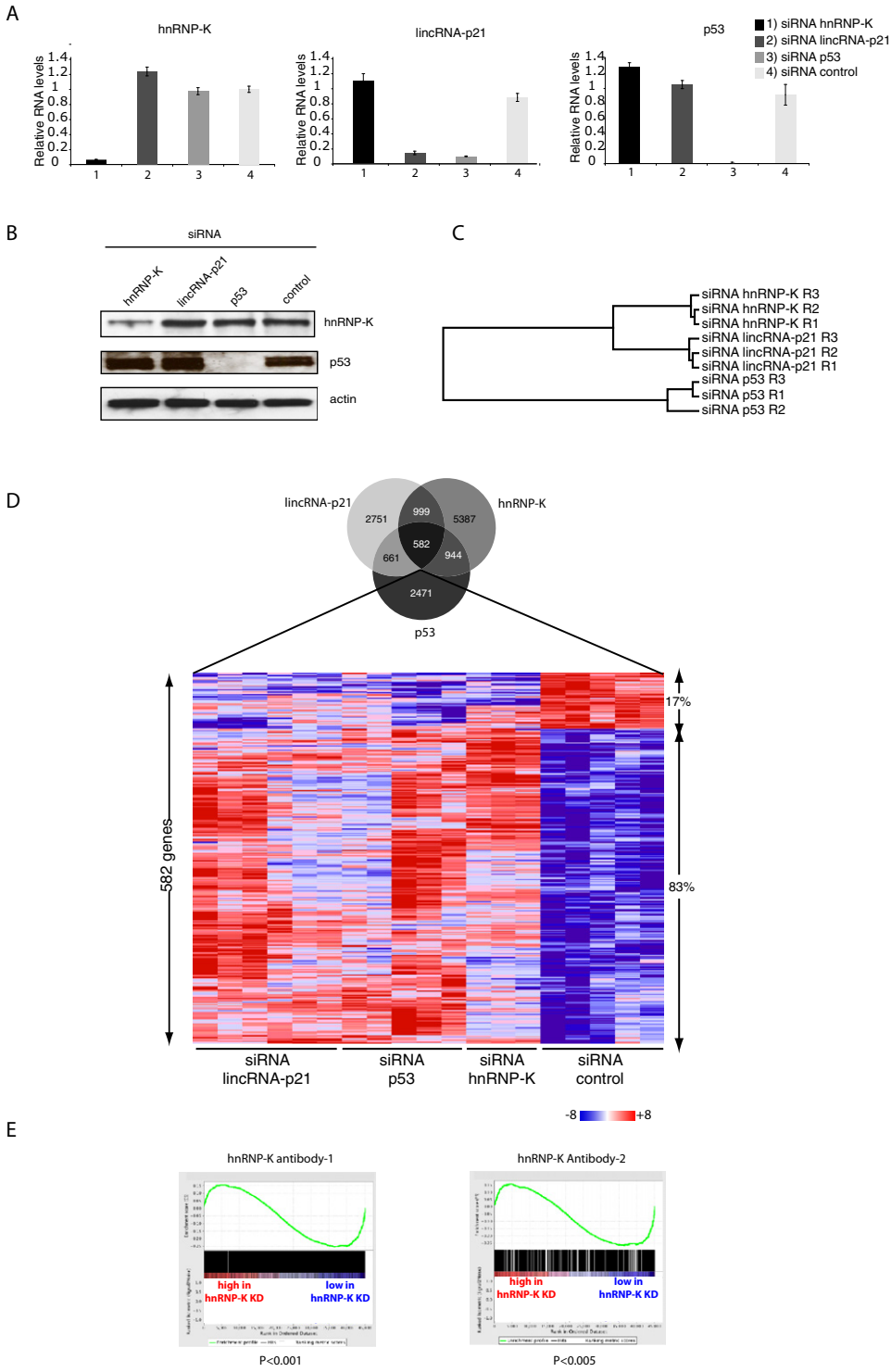

Figure S6. LincRNA-p21, p53 and hnRNP-K Depletion Results on Derepression of Coregulated Genes, Related to Figure 6

(A) siRNA depletion of hnRNP-K, lincRNA-p21 and p53 in one set of replicates of the samples subjected to microarray analysis. p53-restored $p53^{LSL/LSL}$ MEFs were transfected with siRNA pools targeting hnRNP-K, lincRNA-p21, p53 or a non-targeting siRNA pool. 24 hr after transfection cells were treated with 100nM doxorubicin for 14 hr and then RNA was extracted and analyzed by qRT-PCR for quantification of hnRNP-K (left panel), lincRNA-p21 (middle panel) and p53 (right panel) RNA levels. Values are the median of 4 technical replicates +/−STD.

(B) hnRNP-K and p53 protein levels in lincRNA-p21, hnRNP-K, p53 and control siRNA treated cells. p53-restored $p53^{LSL/LSL}$ MEFs were treated as in (A), protein was extracted and levels of hnRNP-K (top panel) and p53 proteins (middle panel) were determined by Western blot analysis. The bottom panel shows beta-actin

levels as loading control.

(C) Hierarchical clustering of the genes differentially expressed (FDR < .05) in either one of the three siRNA treatments (lincRNA-p21, p53 or hnRNP-K). Cells were treated like in (A). Three biological replicates (R1, R2 and R3) were included for each siRNA treatment and differentially expressed genes were determined by microarray analysis (FDR < 0.05) (Supplemental Experimental Procedures).

(D) LincRNA-p21, p53 and hnRNP-K depletion result on derepression of many coregulated genes. Top: Venn diagram representing the number of genes affected by. lincRNA-p21 (top left), hnRNP-K (top right) or p53 (bottom) siRNA-depletion. The central intersection represents the genes commonly regulated by lincRNA-p21, hnRNP-K and p53 relative to the control siRNA (FDR < 0.05). Bottom: Relative expression values of the set of genes coregulated by lincRNA-p21, p53 and hnRNP-K in each experimental condition. Data from two independent experiments with 3 and 2 biological replicates per experiment respectively are included for lincRNA-p21, p53 and control siRNAs. Data from one experiment and 3 biological replicates are included for hnRNP-K siRNA. Transcripts above or below the global median are represented in shades of red and blue respectively (shades of red and blue are scaled to 8 fold activation and repression respectively).

(E) hnRNP-K binds to the genes affected by hnRNP-K siRNA-depletion. GSEA analysis comparing the genes missregulated upon hnRNP-K knockdown (FDR < .05) with the genes whose promoters are bound by hnRNP-K protein in two independent ChIP-chip experiments. ChIP-chip with hnRNP-K monoclonal antibody (left) or hnRNP-K polycolonal antibody (right panel).